Genipin-crosslinked gelatin microspheres as a strategy to prevent postsurgical peritoneal adhesions: in vitro and in vivo characterization

Kaat De Clercq[a], Charlotte Schelfhout[a], Marc Bracke[b], Olivier De Wever[b], Mieke Van Bockstal[c], Wim Ceelen[d], Jean Paul Remon[a] , Chris Vervaet[a,*]

[a] Laboratory of Pharmaceutical Technology, Ghent University, Belgium
[b] Laboratory of Experimental Cancer Research, Ghent University, Belgium
[c] Department of Pathology, Ghent University Hospital, Belgium
[d] Department of Surgery, Ghent University Hospital, Belgium

---

ABSTRACT

Background. Peritoneal adhesions are a common complication after abdominal surgery. They cause small bowel obstruction, female infertility and chronic abdominal pain. Peritoneal adhesions also hamper uniform drug distribution in the peritoneal cavity, thereby reducing the efficacy of intraperitoneal chemotherapy after cytoreductive surgery.

Aim. The goal of this study was to develop a formulation that prevents peritoneal adhesions, evenly distributes in the abdominal cavity, and simultaneously extends residence time and improves local drug concentration. This report describes the formulation and characterization of genipin-crosslinked gelatin microspheres (GP-MS).

Methods and results. Spheroid gelatin microspheres were prepared by an emulsification solvent extraction method. A higher degree of crosslinking was obtained by increasing genipin concentration and crosslinking time. The degree of crosslinking allowed to tailor the degradation rate of GP-MS, hence their residence time. GP-MS did not affect cell viability. In vivo experiments showed excellent GP-MS biocompatibility and degradation characteristics. GP-MS were distributed evenly throughout the abdominal cavity. Adhesions were induced in Balb/c mice by application of an abraded peritoneal wall-cecum model. GP-MS-treated mice developed significantly less postsurgical adhesions compared to saline and Hyalobarrier® group. Histopathological examination showed a decrease of peritoneal inflammation over time in GP-MS-treated mice with complete recovery of peritoneal wounds post-operative day 14.

Conclusion. GP-MS are a promising strategy to prevent postoperative peritoneal adhesions and improve efficacy of postoperative intraperitoneal chemotherapy.

Keywords: *microspheres*
crosslinking
genipin
peritoneal adhesions prevention
post-operative adhesions
anti-adhesion barrier

*Corresponding author. Laboratory of Pharmaceutical Technology, Ghent University, Ottergemsesteenweg 460, 9000 Ghent, Belgium. Tel.: +32 9 264 80 69, fax: +32 9 222 82 36. E-mail address: chris.vervaet@ugent.be

1. Introduction

Peritoneal adhesions are defined as pathological attachments between tissues and organs, usually between the omentum, bowel loops and the abdominal wall. They can be classified as congenital or acquired[1]–[3]. The majority of adhesions is acquired and can be subdivided according to their inflammatory or postsurgical etiology. Inflammatory adhesions result from the inflammatory response of the peritoneum during intra-abdominal inflammatory processes such as acute appendicitis, pelvic inflammatory disease and exposure to intestinal contents[1]–[3]. Postsurgical adhesions develop when injured tissue fuse together to form scar tissue[1]–[4]. The reported incidence of intraperitoneal (IP) adhesions varies from 67 to 93% after general intra-abdominal surgery and up to 97% after open gynaecologic surgery[1]–[3],[5]. Peritoneal adhesions affect quality of life by causing small bowel obstruction, female infertility, chronic abdominal pain and inadvertent organ injury after reoperative surgery [1]–[7].

Severe peritoneal adhesions are often observed after major surgery for abdominal malignancies. Cytoreductive surgery followed by IP chemotherapy is becoming the standard of care for patients with advanced cancers such as colorectal or ovarian tumours. Peritoneal carcinomatosis results from dissemination of primary intra-abdominal and gynecological cancers[8]–[14]. The effectiveness of IP chemotherapy depends on uniform drug distribution in the peritoneal cavity as well as on the concentration and exposure time of residual tumours to the instilled drugs. Adhesions occuring after cytoreductive surgery can compromise the effect of IP chemotherapy[15]–[17]. Therefore, a formulation that distributes evenly in the abdominal cavity, prevents peritoneal adhesions and simultaneously extends residence time and enhances local drug concentration is of high clinical interest. Biocompatible microspheres might be suitable candidates to meet these objectives.

Microparticles for IP drug delivery are promising since they can overcome some major challenges. They can distribute throughout the entire peritoneal cavity. Due to their size, they can remain in the peritoneal cavity and locally provide an extended release of a drug, such as a chemotherapeutic agent[16], [18]–[21]. The size range of the microspheres is crucial as size determines the residence time in the peritoneal cavity. Small particles can be cleared from the peritoneal cavity into the lymphatic capillaries through openings in the diaphragm (stomata), or they can be absorbed through the peritoneal membrane. The stoma openings are 3-12 μm in diameter and provide a direct access to the underlying submesothelial lymphatic system, allowing rapid removal of cells, fluid, bacteria and particles from the peritoneal cavity. Particles with a larger diameter are longer retained in the peritoneal cavity. Particle size will also affect drug release rate as smaller particles release the drug faster, due to their higher surface area-to-volume ratio. Furthermore, particle size will affect the spatial distribution in the abdominal cavity. Previous studies show that smaller microparticles are evenly distributed throughout

the abdominal cavity whereas larger microparticles are mainly localized in the lower abdomen[16], [18], [20], [22]–[25].

Microspheres for IP use should not cause an inflammatory reaction, nor should they have an intrinsic tendency to create peritoneal adhesions. Inflammation is dependent on the type of material and the particle size[15],[24]. The use of biocompatible and biodegradable polymers such as gelatine and collagen might overcome toxicity and biodegradability problems, which are related to the use of synthetic materials[26].

Gelatin is an ideal candidate to formulate biocompatible microspheres. It has excellent film- and particle-forming capacities, as well as bioadhesive properties. Gelatin is not toxic or carcinogenic, and it is a readily available and inexpensive material. As a result, gelatin has been extensively used for medical, pharmaceutical and cosmetic applications[26]–[30]. However, its rapid dissolution in an aqueous environment under *in vivo* conditions requires the use of crosslinkers for long-term biomedical application of gelatin microspheres[26], [27], [29], [30].

The selection of a chemical crosslinking agent is critical since residual crosslinking agent in the formulation can cause toxic side effects. Numerous chemical reagents have been used including glutaraldehyde, formaldehyde, diepoxide and 1-ethyl-3-(3-dimethylaminopropyl)carbodiimide[28], [30]–[32]. Genipin, a naturally occurring crosslinker, isolated from the fruits of the plant *Gardenia jasminoides*, is superior to other chemical crosslinking agents as it is 10 000 times less toxic than aldehyde and epoxy crosslinkers. Furthermore, genipin improves both thermal and structural stability of crosslinked gelatin since the degradation rate of genipin-crosslinked gelatin microspheres was significantly slower compared to aldehyde as crosslinker. Therefore, genipin is a promising crosslinking agent to formulate a long-acting biomedical implant[27], [32]–[35].

This study presents the formulation and *in vitro* and *in vivo* characterization of genipin-crosslinked gelatin microspheres. The aim of this study is to develop a formulation that evenly distributes in the peritoneal cavity. The potential efficacy of genipin-crosslinked gelatin microspheres to prevent postsurgical peritoneal adhesions is evaluated in a standardised mouse model[17].

2. Materials and methods

2.1 Formulation of gelatin microspheres

Gelatin microspheres were prepared by a modified emulsification solvent extraction method as reported by Adhirajan et al. (2007)[28]. 10 ml of a gelatin (Gelatin Type B, Rousselot, Ghent, Belgium) aqueous solution was added dropwise at 60°C to 100 ml of peanut oil (Fagron, Waregem, Belgium) pre-heated to 60°C. Various concentrations (5, 10, 15, 20, 25 and 30 % (w/v)) and gelatin grades (75, 100, 160, 200, 250 and 265 bloom) of gelatin were evaluated to obtain the appropriate size of the microspheres. The influence of the addition of surfactants to the size of microspheres was also investigated. A concentration of 0.1 wt% of surfactant (Tween®20 (Fagron), Tween®80 (Fagron,), Tween®85 (Sigma-Aldrich, Bornem, Belgium), Pluronic®L121 (BASF, Ludwigshafen, Germany), Pluronic®F127 (Sigma-Aldrich), Pluronic®F68 (Sigma-Aldrich), Cremophor®RH60 (BASF)) was added to the oil phase. A combination of two surfactants was evaluated where 0.1 wt% of surfactant A (Tween®80, Span®85 (Sigma-Aldrich)) was added to the aqueous phase and 0.1 wt% of surfactant B (Span®80, Tween®85 (Sigma-Aldrich)) to the oil phase. The two phases were emulsified for 15 minutes at 900 rpm using a magnetic stirrer. The emulsion was then rapidly cooled to 5°C in an ice bath and stirring continued for 20 minutes to allow the spontaneous gelation of the gelatin aqueous solution. The microspheres were dehydrated by the addition of 150 ml precooled acetone (Sigma-Aldrich) and stirring was continued for 30 minutes. The microspheres were collected by filtration using a cellulose filter (Whatman filter grade 4) and a vacuum pump. The microspheres were washed several times with acetone to remove residual oil from their surface. The washed microspheres were finally vacuum-dried at room temperature for at least 2 days.

2.3 Crosslinking of gelatin microspheres

Gelatin microspheres were crosslinked using various genipin (Wako Chemicals, Neuss, Germany) concentrations and crosslinking times[33]. The prepared gelatin microspheres (500 mg) were dispersed in 10 ml 90% v/v ethanol (Sigma-Aldrich) solution containing different genipin concentrations (0.1, 0.5 and 1% w/v) and stirred at room temperature using a magnetic stirring for different time periods (5, 15, 24, 48, 72, 96 h). At the end of incubation, the genipin solution was aspirated and the crosslinked gelatin microspheres were rinsed with 15 ml aqueous ethanol solution (99.5% v/v) for 4 hours to remove residual genipin. Subsequently, the rinsed microspheres were filtered from the ethanol solution and vacuum-dried at room temperature for 24 h to remove ethanol.

2.4 Characterization of microspheres

The morphology of gelatin microspheres in dispersed state was examined by optical microscopy (Leica DM2500 P).

Particle size and size distribution of the microspheres dispersed in water were measured in triplicate by laser diffraction analysis using a Mastersizer 2000 (Malvern Instruments, Malvern, Worcestershire, UK). The wet dispersion cell of the Mastersizer 2000 (Hydro 2000SM; Malvern Instruments, Malvern, Worcestershire, UK) was used. D(v, 0.1), D(v, 0.5) and D(v, 0.9) define the particle size of the volume distribution in microns where 10, 50 and 90%, respectively, of the particles are smaller than this diameter.

2.5 Evaluation of the degree of crosslinking

A ninhydrin assay was performed to determine the degree of crosslinking by comparing the percentage of free amino groups in genipin-crosslinked gelatin microspheres and uncrosslinked gelatin microspheres[29], [35]. The ninhydrin reagent consisted of two solutions. Solution A contained 1.05 g citric acid (Fagron), 0.4 g NaOH (Sigma-Aldrich) and 0.04 g $SnCl.H_2O$ (Sigma-Aldrich) dissolved in 25.0 ml water. Solution B was made by mixing 1.0 g ninhydrin (Sigma-Aldrich) with 25.0 ml ethylene glycol monomethyl ether (Fisher Scientific, Erembodegem, Belgium). Solutions A and B were combined and stirred for 45 min in the dark at room temperature. Solutions of known concentrations of glycine (Sigma-Aldrich) were prepared to generate a standard curve. Uncrosslinked and crosslinked microspheres were lyophilized prior to analysis. Samples of 3 mg lyophilized microspheres were weighed and rehydrated in 100 µL water. 1.0 ml ninhydrin solution was added to the samples and standard solutions, followed by incubation at 100°C for 20 min in the dark. Next, the samples were cooled to room temperature and 5.0 ml 50% isopropanol (Fisher Scientific) was added to each sample. The optical absorbance of the solutions at 570 nm was recorded with a spectrophotometer (UV-1650PC, Shimadzu Benelux, Antwerp, Belgium). The amount of free amino groups in the sample, after heating with ninhydrin, is proportional to the optical absorbance of the solution. The concentration of free NH_2 groups in the sample is determined from a standard curve of glycine concentration versus absorbance. The degree of crosslinking of the sample is calculated following the equation:

$$\text{degree of crosslinking} = \frac{(\text{NHN reactive amine})_{\text{non-crosslinked}} - (\text{NHN reactive amine})_{\text{crosslinked}}}{(\text{NHN reactive amine})_{\text{non-crosslinked}}}$$

where 'non-crosslinked' is the mole fraction of free NH_2 in non-crosslinked samples and 'crosslinked' is the mole fraction of free NH_2 remaining in crosslinked samples. Each measurement was performed in triplicate.

2.6 Evaluation of in vitro degradation

An *in vitro* enzymatic degradation test was carried out using collagenase[27], [28], [32]. Fifty mg of microspheres was suspended in 5 ml reaction buffer containing 50 mM Tris (Sigma-Aldrich), 2 mM $CaCl_2$ (Sigma-Aldrich), 20 U/ml collagenase type I (Sigma-Aldrich) and incubated at 37°C for 48 h. Samples of 200 µL were taken after 5, 24 and 48 h. 200 µl of quenching buffer (12% w/v PEG 6000 (Sigma-Adrich) and 25 mM EDTA (Fagron) in water) was added to prevent further degradation. Ninhydrin assay was performed to quantify the percentage of degradation[36]. 2 ml of ninhydrin solution, prepared as described in section 2.5, was added to the samples. The reaction was carried out at 100°C for 10 minutes in the dark. Samples were cooled to room temperature and 2 ml 50% v/v isopropanol (Fisher Scientific) was added. Optical absorbance of the solutions was measured at 570 nm using a spectrophotometer (UV-1650PC, Shimadzu Benelux, Antwerp, Belgium). The absorbance at 570 nm was proportional to the amount of degradation. An increase in degradation resulted in more free amino acids and therefore higher absorbance. Percentage of degradation was compared to degradation of non-crosslinked gelatin microspheres.

A hydrolytic degradation study was performed by dispersing uncrosslinked and genipin-crosslinked gelatin microspheres (GP-MS) in 5 ml phosphate buffered saline (PBS) and incubated at 37°C for the duration of the study. The morphology of the microspheres was daily observed using optical microscopy (Leica DM2500 P)[37].

2.7 In vitro cell viability

The human ovarian carcinoma cell line (SKOV-3, obtained from the American Type Culture Collection) was cultured at 37°C in a 5% CO_2-containing humidified atmosphere in McCoys medium (Invitrogen, Merelbeke, Belgium). Medium was supplemented with 10% fetal bovine serum, penicillin, streptomycin (Invitrogen) and fungizone (Bristol Myers Squibb, Braine-l'Alleud, Belgium).

To test the cytotoxicity of the crosslinker a broad range of genipin concentrations was evaluated (0.0001, 0.001, 0.005, 0.01, 0.05, 0.1, 0.5, 1, 5 % w/v), and an MTT assay was performed after 24, 48, 96 h and 1 week of incubation. To evaluate the cytotoxicity, 30×10^3, 25×10^3, 20×10^3 and 10×10^3 cells/well were seeded in 96-well plates (Starstedt, Newton NC, USA). After 48 h, 20 µl medium was replaced by 20 µl genipin solution. After 24 h, 48 h, 96 h or 1 week incubation at 37°C under 5% CO_2-atmosphere, medium was entirely removed, cells were washed three times with PBS and 200 µL medium was added to each well. The cytotoxicity of GP-MS was tested at 0.1, 1.0 , 2.5, 5.0, 10, 25 and 50 mg/ml. 30×10^3, 25×10^3, 20×10^3, 10×10^3 and 5×10^3 cells/well were seeded in 96-well plates for incubation with the formulation during 24 h, 48 h, 96 h, 1 week or 2 weeks, respectively. After 48 h, 20 µl medium was replaced by 20 µl formulation. After the required incubation period at 37°C under 5% CO_2-atmosphere, the medium was entirely removed, cells were washed three times with PBS and 200 µL

medium was added to each well. Six wells per concentration were used and all experiments were performed in triplicate. Cell viability was determined via the MTT assay and compared with non-treated cells.

The MTT assay was performed by replacing 100 µl medium by 100 µl MTT-reagent (3-(4,5 dimethylthiazol-2-yl)-2,5-difenyl-tetrazolium bromide) (Sigma-Aldrich) at a concentration of 1 mg/ml in PBS-D^+ (Thermo Fischer Scientific). The plates were incubated in the dark for 2 h at 37°C and 5% CO_2-atmosphere. Afterwards, all medium was removed and 200 µL DMSO (Acros Organics, Geel, Belgium) was added to dissolve formazan crystals. Optical density was measured at 570 nm, normalizing with a reference wavelength of 650 nm using an ELISA-plate reader (Paradigm Detection Platform, Beckman Coulter, Suarleé Belgium).

Genipin leaching, the amount of genipin released from the microspheres, was evaluated. 50 mg of GP-MS (0.5% wt genipin; 5, 15, 24, 48, 72 and 96 h of crosslinking) were immersed in 5 ml PBS at 37°C. Genipin leaching over time was analysed by measuring optical absorbance of supernatans at 240 nm.

2.8 Animal study

All animal experiments were approved by the Ethical Committee of the Faculty of Medicine, Ghent University (ECD 14/11). Female Balb/c mice (Envigo, Horst, The Netherlands) were kept in standard housing conditions with water and food *ad libitum* and a 12 hours light/dark cycle.

2.8.1 In vivo biocompatibility, degradability and toxicity study

15 Balb/c mice, aged 6 weeks, received an IP injection of the formulation into the left lower quadrant. GP-MS were sterilised in ethanol solution prior to administration. 50 mg sterilised gelatin microspheres, crosslinked using 0.5% w/v genipin for 48 h, were suspended in 2 ml sterile physiological saline (Baxter, Lessines, Belgium) and injected. All animals were observed after administration of the formulation, including general condition (activity, energy, hair, faeces, behaviour pattern and other clinical signs), body weight and mortality. After 2, 7, 14, 21 and 28 days three mice per time point were sacrificed by cervical dislocation under anaesthesia with sevoflurane (Sevorane®, Abbott, Waver, Belgium). A vertical incision along the midline through the abdominal wall muscle and peritoneum was made and the abdominal cavity was exposed. Distribution, compatibility and degradability of GP-MS were examined. The abdominal cavity was photographed. Specimens of cecum, colon, greater omentum and parietal peritoneum were assigned for histopathological examination to evaluate local tolerance. Specimens of spleen, pancreas, liver and kidneys were taken to evaluate general toxicity. Tissues were fixed immediately by immersion in 4% paraformaldehyde in PBS for 72 hours and embedded in paraffin. The tissues were then sectioned, stained with hematoxylin and eosin (H&E). All slides were examined for tissue inflammatory reaction by a pathologist in a blinded manner.

2.8.2 Effectiveness of gelatin microspheres in prevention of postoperative peritoneal adhesions

2.8.2.1. Influence of GP-MS to the mechanism of adhesion formation over time

15 Balb/c mice, aged 6 weeks, were sedated by inhalation anaesthesia with sevoflurane, induction 8% and maintenance 3%. Prior to anaesthesia, mice received a subcutaneous injection of buprenorphine 0.05 mg/kg (Temgesic®, Schering-Plough, Heist-op-den-Berg, Belgium). Body temperature was controlled using a heating plate.

Peritoneal adhesions were induced by the abdominal wall and cecum abrasion peritoneal adhesion model as previously reported[17], [38], [39]. An anterior midline incision was made through the abdominal wall and peritoneum. The cecum was identified and abraded until visible damage by scrubbing with sterile dry surgical gauze. The damaged cecum was returned to the abdominal cavity and a 1x1 cm apposing parietal peritoneal wall defect was created using a sterile dry gauze. No attempt of hemostasis or IP irrigation was made. The abraded cecum was placed in apposition to the peritoneal wall defect. Then, the incision was closed in two layers with a PDS II 6/0 suture (Ethicon®, Johnson & Johnson, Sint Stevens Woluwe, Belgium).

After complete closure, 12 Balb/c mice (GP-MS-treated mice) were intraperitoneally injected in the left lower quadrant with the formulation. Fifty mg of GP-MS, crosslinked using 0.5% w/v genipin for 24 h and sterilised by immersion in ethanol solution, were dispersed in 2 ml of sterile physiological saline (Baxter) and injected. Three Balb/c mice (control mice) received an IP injection of 2 ml of physiological saline (Baxter) in the left lower quadrant. Mice were checked daily for changes in behaviour (feeding, grooming, etc.) and body weight was monitored.

The anti-adhesion efficacy of GP-MS was evaluated 2, 7 and 14 days post-operative, 3 GP-MS-treated mice and 1 control mouse per time point. Mice were sacrificed by cervical dislocation under anaesthesia with sevoflurane. Abdominal cavity was exposed and tissues were investigated on typical inflammatory signs. Adhesions were qualified and quantified using standard scoring systems**.** The qualitative adhesion scoring (Table 1) was based on extent, type and tenacity of adhesions, as described by Binda et al. (2007)[40], [41] with some modifications.

The extent of adhesion was assessed by the area of the peritoneal cavity that was covered by adhesions. Therefore, the abdominal cavity was hypothetically subdivided into 8 sections, each consisting 12.5% of abdominal area, as illustrated in Figure 1[41], [42].

Adhesions were assessed according to the quantitative scoring system reported in Egea et al. (1995) with some modifications[42] as displayed in Table 2.

Specimens for histopathological examination were taken from the cecum, abdominal wall and, if applicable, adhesion tissue. The tissues were fixed immediately by immersion in 4% paraformaldehyde in PBS for 72 h and embedded in paraffin. The tissues were then serially sectioned, stained with H&E and analyzed using light microscopy by a pathologist in a blinded manner.

2.8.2.2 . Proof of concept: effectiveness of GP-MS in the prevention of postsurgical peritoneal adhesions in a standardized mouse model

A large scale study was performed to compare the effectiveness of GP-MS to the commercially available Hyalobarrier® gel (n=11) (Anika Therapeutics, Abano Terme, Italy) in the prevention of postsurgical peritoneal adhesion formation in a standardized mouse model. Mice of the control group (n=11) were only treated with saline. Mice were at random assigned to control, GP-MS or Hyalobarrier® group.

Peritoneal adhesions were induced by the abdominal wall and cecum abrasion peritoneal adhesion model as described above. After complete closure of the anterior midline incision, 2 ml of 0.9% NaCl (Baxter) or 50 mg GP-MP dispersed in 2 ml of 0.9% NaCl were IP injected in the left lower quadrant of 11 Balb/c mice in the control and GP-MP arm, respectively. Gelatin microspheres, crosslinked for 24 h in 0.5% m/v genipin, sterilized by immersion in 96% v/v ethanol (Sigma-Aldrich) solution for 4 hours prior to IP administration. Hyalobarrier® gel (4% ACP, Anika Therapeutics) (n=11) was applied in a thin layer to the lateral and ventral surface of the damaged cecum and the 1x1 cm parietal peritoneal defect before closure of the abdomen according to the manufacturer's instructions. All proceedings were performed under clean conditions by one surgeon in a blinded way. Mice were monitored for recovery from anesthesia and their general conditions and body weight were followed daily.

At day 14 a second ventral laparotomy was performed, the abdominal cavity was exposed and tissues were investigated on typical inflammatory signs. In addition, adhesions were qualified and quantified in a blinded manner using three scoring systems. Qualitative adhesion scoring was based on extent, type and tenacity of adhesions, as described by Binda et al. (2007) with some modifications[40], [41] as displayed in Table 1. Adhesions were assessed according to the quantitative scoring system reported in Egea et al. (1995) with some modifications[41], [42] as displayed in Table 2. Additionally, adhesions were graded (Table 3) according to the Zühlke grading classification[41], [43].

Specimens for histopathological examination were taken from the cecum, abdominal wall and, if applicable, adhesion tissue. The tissues were fixed immediately by immersion in 4% paraformaldehyde in PBS for 72 h and embedded in paraffin. The tissues were then serially sectioned, stained with H&E and analyzed using light microscopy by a pathologist in a blinded manner.

Blood samples were obtained from the tail vein of mice prior to induction of adhesions, at day 1 and 7 postoperative. At day 14 blood was obtained by intracardiac puncture using a 27 G needle and mice were sacrificed by cervical dislocation under anesthesia sevoflurane. The blood samples were centrifuged at 2500 rpm during 10 minutes. Additionally, peritoneal lavages were performed at day 0, 1, 7 and 14. Five ml of cooled PBS was intraperitoneally injected, abdomen was gently massaged and peritoneal fluid was collected. Quantification of cytokines interleukin (IL) 1ß, IL-6 and TNF-α in plasma and peritoneal fluid was performed using ELISA kits (Qiagen, Antwerp, Belgium).

Statistical analysis were performed using the nonparametric Wilcoxon-Mann Whitney test in GraphPad Prism™ version 5.2 to compare the total adhesion score, grade and extent of adhesion between each pair of treatment groups. The incidence of adhesions was compared using the Fisher's Exact test. A P-value < 0.05 on a two-tailed test was considered to be statistically significant.

3. Results and discussion

3.1 Formulation of gelatin microspheres

The size of gelatin microspheres can be controlled by adjusting the concentration of gelatin in the aqueous phase. A higher gelatin concentration increases the size of the aqueous droplets in emulsion and thus the size of the final gelatin microspheres. Nevertheless, a minimum viscosity is necessary for a good emulsification process as no microspheres or microspheres with a poor morphology were formed when an aqueous gelatin solution of 5 and 10 w/v % was used. A gelatin with a high gel strength (i.e. bloom value of 265) was selected as this gelatin grade yielded microspheres with a better spherical morphology in comparison to gelatin grades with bloom values of 160, 200 and 250. Microspheres were not formed when a gelatin grade of 75 and 100 bloom was used. Aggregation tendency of the microspheres depended on the bloom value of gelatin: less aggregation was observed at higher bloom value. Addition of surfactants also controls the size of microspheres by reducing the size and the aggregation tendency of the gelatin droplets during the emulsification process[26]. Figure 2 displays laser diffraction results, illustrating how the final microspheres size can be managed by the concentration of the gelatin solution and the addition of a surfactant.

The influence of different types of surfactants, i.e. sorbitan esters (Span®) and their ethoxylates (Tween®), poloxamers (Pluronic®) and polyethoxylated castor oil (Cremophor® RH), on the size of microspheres was investigated. The influence of the surfactants on the size of the microspheres is displayed in Table 4, presenting the volume mean diameter, D[4,3]. The addition of 0.1 wt% Cremophor® RH 60 (polyoxyl 60 hydrogenated castor oil) to the oil phase resulted in the smallest microspheres with a narrow size distribution, low aggregation tendency and good spheroid morphology.

Microspheres with a size of about 50 µm were selected for further experiments based on their intended use for IP administration since smaller sized microspheres are more easily to inject intraperitoneally. To obtain microspheres of 50 µm, 15 w/v% gelatin (265 bloom) solution was added dropwise to 100 ml of peanut oil with 0.1 wt% Cremophor®RH60, emulsified and extracted as described above. The obtained microspheres had a volume mean diameter, D[4,3], of 58 ± 10 µm and a span of 1.22 in the dispersed state. A spherical morphology of the microspheres without tendency towards aggregation was observed.

3.2 Crosslinking of gelatin microspheres

Gelatin microspheres were crosslinked using genipin in various concentrations and crosslinking times. Blue coloration increased with higher genipin concentration and a longer incubation time: ninhydrin assay confirmed that a higher degree of crosslinking is obtained when increasing genipin concentration and crosslinking time (Figure 3).

Genipin can react with the free amino groups of lysine, hydroxylysine and arginine residues in proteins to form intra- and intermolecular crosslinks. The reaction between a genipin and an amino acid in gelatin is initiated by a nucleophilic attack of the amino group on the third carbon of genipin. The genipin ring is opened and an aldehyde group is formed. The resulting aldehyde group is attacked by the attached secondary amine group. Further radical reaction leads to dimerization. Hence, genipin may link peptide chains by introducing a dimeric genipin spacer with a cyclic structure. Consequently, genipin can form intramolecular crosslinks within a gelatin molecule and short-range intermolecular crosslinks between two adjacent gelatin molecules[27], [29], [44]. Intermediates formed during the crosslinking reaction are linked to the blue coloration. Some suggest that genipocyanin is a major component, a result of a 1:1 reaction between genipin and amino acid. Spontaneous reaction of genipin as azaphilone with an amino group forms a nitrogen-iridoid which undergoes dehydration to form an aromatic monomer[45]. Others speculate that genipin molecules may be polymerized before crosslinking with amino groups[31].

Crosslinking gelatin microspheres did not induce changes in morphology or size. Photographs of GP-MS in the dispersed state are displayed in Figure 4. Microspheres crosslinked during 5 h and 24 h had a mean volume diameter of 57.11 ± 5.03 μm (n=3) and 55.53 ± 5.08 μm (n=3), respectively.

3.3 In vitro degradation

The degradation mechanism of the microspheres is probably a combination of hydrolysis and proteolysis. Therefore, two types of degradation assays were performed. Proteolysis can be accelerated in case of metastasis as it has been noticed that tumour cell invasion and metastasis are related to a higher expression of degrading enzymes, such as heparanase, serine protease, thiol protease and metal-dependent enzymes. A shift in proteolytic balance of proteases facilitates the matrix modulation in the metastatic cascade. Tumour cells can directly secrete degrading enzymes or induce proteinase activity in neighbouring cells. Matrix metalloproteinases (MMP) play an important role in extracellular matrix degradation. MMP collagenase I was chosen as model enzyme as it is most widely expressed. Collagenase I is secreted by both normal cells, eg. stromal fibroblasts, macrophages, endothelial and epithelial cells, as well as by tumour cells[46]–[49]. The *in vitro* proteolytic study allowed a rapid evaluation of the biodegradability. Enzymatic degradation properties of microspheres are displayed in Figure 5. All microspheres were degraded within 48 hours. An increase in degree of crosslinking and genipin concentration resulted in a longer resistance to enzymatic degradation.

The resistance of GP-MS to hydrolysis was evaluated (Table 5). Microspheres longer remained intact when a higher genipin concentration and longer duration of crosslinking was used. Microspheres crosslinked with 0.1 w/v % genipin were all degraded within 8 days, whilst using concentrations of 0.5 and 1.0 w/v % genipin increased the resistance of microspheres to degradation. Microspheres crosslinked for 96 h with 1.0 w/v % genipin remained intact for about 60 days.

The degree of crosslinking allowed to tailor the degradation rate of microspheres and thus their residence time.

3.4 In vitro cell viability

Previous reports describe low cytotoxicity of genipin as crosslinking agent in comparison to aldehyde crosslinkers[27], [32]–[35]. This study evaluated the influence of genipin on cell viability of SKOV-3 cells. Both concentration- and time-dependent influence of the crosslinking process on cell viability are evaluated since the gelatin microspheres are intended to be retained for a prolonged period in the peritoneal cavity (Figure 6A).

MTT assays clearly indicated that genipin influenced cell viability at high concentrations. Concentrations of 0.5 w/v % and higher caused a steep decrease of cell viability after one day of incubation. Cell viability decreased further in time to a minimum of 20%. Acute cytotoxicity was noticed with a minimum cell viability of 25% after 48 h of exposure to 0.5 w/v % genipin. Surprisingly, cells seemed to recover in time which could reflect the loss of cell-cell contacts and mitochondrial reactivation[50], [51]. Low genipin concentrations (0.0001 to 0.01 w/v %) hardly had an effect on cell viability, while concentrations of 0.05 and 0.1 w/v % affected cell viability with a gradual decrease in function of time. Hence, only the lowest genipin concentrations (0.0001 to 0.005 w/v %) can be considered as non-cytotoxic. Since the cytotoxicity of genipin is determined by the free concentration of the crosslinker exposed to cells, leaching of genipin from microspheres was evaluated. The amount of genipin released from the microspheres was very low and within the non-cytotoxic concentration range. Measured genipin concentrations ranged from 0.00007 w/v % (70% degree of crosslinking) to 0.001 w/v % (40% degree of crosslinking) and 0.004 w/v % (<40% degree of crosslinking). Based on the aforementioned cytotoxicity data, it is hypothesised that the free genipin released from the microspheres will not affect cell viability. The low amount of genipin released from the crosslinked microspheres is linked to the stable nature of the inter- and intramolecular crosslink [27], [31], [44].

This hypothesis was confirmed by performing a new set of MTT assays where SKOV-3 cells were exposed to several concentrations of GP-MS with a degree of crosslinking of 60%. Figure 6B indicates that cell viability was not affected by the presence of GP-MS. Neither exposure time nor concentration of GP-MS had an influence on cell viability.

3.5 Animal study

3.5.1 In vivo distribution pattern, biocompatibility and degradability

Animals were followed during the entire period of the study and all of them tolerated the formulation well. Body weight gain was not different from the standard body weight increase and general activity was normal. The formulation consisted of GP-MS with a 60% degree of crosslinking using 0.5 w/v % genipin as crosslinking concentration. A high degree of crosslinking was chosen to

ensure a long retention time in the peritoneal cavity in order to obtain information on the short and longer term inflammatory and toxicity responses.

The distribution of GP-MS in the abdominal cavity was visually evaluated (Figure 7) based on the blue colour of the particles. The microspheres displayed a distribution pattern similar to the flow of peritoneal fluid. The gelatin microspheres distribute throughout the whole abdominal cavity, from injection site to colon, cecum, omentum, diaphragm and liver, and accumulation of the formulation at the typical sites of peritoneal carcinomatosis was seen. The peritoneal carcinomatosis pattern has been described and tumour growth was predominantly found in the following locations: in the small pelvis, at the end of the ileal mesentery, at the sigmoid colon, and at the right paracolic gutter (cecum, ascending colon)[52], [53]. Thus, the distribution pattern of the microspheres is an attractive characteristic in view of its intended use for drug delivery in the treatment of peritoneal carcinomatosis. Upon examination of the abdominal cavity and organs there were no visible signs of inflammation or intolerance caused by the presence of the formulation. Previous studies showed that biodegradable poly-(lactic-co-glycolic) acid microspheres with a size range of 5 to 250 μm caused peritoneal adhesions and chronic inflammation after IP injection whilst nanoparticles caused fewer adhesions but were rapidly cleared from peritoneal cavity [24]. All tissues had a normal, healthy appearance and there were no adhesions observed after IP injection of GP-MS. Histopathological examination of the tissues confirmed that there were no signs of inflammation nor intolerance (Suppl. Figure 1a and 1b). No abnormalities were observed in colon, cecum, greater omentum, parietal peritoneum and spleen, liver, pancreas or kidneys compared with the control group. To our knowledge, microspheres for IP administration that do not cause inflammation or intolerance have not yet been described. Nanoparticles are mainly used to achieve these requirements[24], [54], [55]. Since they suffer from rapid clearance, incorporation of nanoparticles into hydrogels has been reported[54].

The formulation remained intact in the peritoneal cavity at day 2, 7, 14 and 21. A gradual decrease of the amount of microspheres over time was noticed, indicating the biodegradation of the formulation. At day 28, only a small amount of microspheres was still present in the abdominal cavity.

3.5.2 Effectiveness in prevention of postoperative peritoneal adhesions

Adhesions were induced by the abdominal wall and cecum abrasion peritoneal adhesion model as has described extensively[6], [17], [38], [56], [57]. The model is highly reproducible and adhesion formation can be easily scored. However, this model might not entirely relate to the clinical appearance of peritoneal adhesions after an abdominal operation, where adhesions are found spread throughout the peritoneal cavity and in between intestines. Nonetheless, the model provides a good indication of the effectiveness of the formulation and allows follow-up of the healing of peritoneum and cecum. GP-MS crosslinked using 0.5 w/v% genipin during 24 h were chosen as formulation to prevent peritoneal adhesions since a degree of crosslinking of 40% ensures complete degradation of the GP-MS within 14

days. Microspheres of 50 μm were chosen for *in vivo* studies since pilot studies using particles of 50, 100, 200 and 300 μm showed that the larger the particles, the more difficult to inject and particles were more evenly distributed in the peritoneal cavity using a smaller particle size.

3.5.2.1. Influence of GP-MS to the mechanism of adhesion formation over time

Scoring of adhesions was conducted 2,7 and 14 days after the induction of adhesions (Table 6). All control mice (Figure 8) developed peritoneal adhesions. Cecum was attached to peritoneal wall (parietal adhesions) and dense adhesions were seen between colon-cecum and small intestines-cecum (visceral adhesions). Sharp dissection was required to separate the adhesions. At day 14, adhesions were vascularised. It is accepted that peritoneal remesothelization is completed by day 8 after peritoneal injury, thus formed adhesions will remain and vascularisation is initiated. Whilst peritoneal adhesions were formed in all control mice, none of the mice treated with GP-MS developed adhesions (Figure 9). At day 2, the formulation was evenly distributed throughout the peritoneal cavity. The microspheres adhered to the affected peritoneum and cecum, forming a barrier to prevent traumatized peritoneal surface apposition during the healing process. No adhesions were found in GP-MS-treated mice 7 days after induction of peritoneal adhesions. GP-MS were completely degraded 14 days after induction of the adhesions, confirming the biodegradability of the formulation. None of the GP-MS-treated mice developed adhesions, peritoneal and cecal injuries appeared healthy and recovered.

Abdominal wall and viscera are covered by a peritoneal layer consisting of mesothelial cells and an underlying extracellular matrix. Peritoneal wounds remesothelialize within 5-6 days for the parietal peritoneum and within 5-8 days for both visceral mesothelium covering the terminal ileum and the mesothelial layer of the parietal peritoneum. The mechanism of adhesion formation can be considered as a variation of the physiological healing process. Injuries to the peritoneum cause a local release of cytokines, IL-1, IL-6 and tumour necrosis factor-α (TNF-α), as a response to trauma. Cytokines attract and activate macrophages to secrete variable substances, including cyclooxygenase and lipoxygenase metabolites, plasminogen activator, plasminogen activator inhibitor (PAI), collagenase, elastase, IL-1 and 6, TNF-α, etc. Postsurgical macrophages recruit new mesothelial cells to lead to peritoneal remesothelialization in response to macrophage-secreted mediators. Formation of the fibrin matrix is of major importance in the adhesion formation cascade. The fibrin clot is formed in several stages from fibrinogen to fibrin monomer, then to soluble fibrin polymer and finally insoluble polymer by coagulation factors. Normally most of the fibrin depositions will disperse by fibrinolysis. The fibrinous mass that remains, results in the organization and formation of adhesions [1], [2].

The balance between deposition and degradation of fibrin will determine normal peritoneal healing or adhesion formation. Fibrinolytic activity usually begins three days after peritoneal injury and increases to a maximum by day 8. Therefore, peritoneal adhesions will remain when remesothelialization is completed by day 8. Normal peritoneum has a high fibrolytic activity to prevent

adhesion formation. But at sites of surgical or inflammatory injury, levels of PAI are increased, which inhibit fibrinolytic activity. Additionally, deficient blood supply and reduced tissue oxygenation, typically for surgical injury, decrease fibrinolysis resulting in adhesion development [1], [2]. Three time points (day 2, 7 and 14) were chosen to evaluate the complete cascade of peritoneal adhesion formation. The microspheres were able to form a barrier between the injured peritoneal surfaces of cecum and parietal peritoneum, thereby hindering the formation of fibrin strands during the remesotheliazation phase. At day 14, when peritoneal healing is completed, adhesions will remain[1], [2]. GP-MS-treated mice did not develop peritoneal adhesions and the peritoneal layer covering abdominal wall and viscera had a normal appearance by day 14. In contrast, control mice developed peritoneal adhesions which were vascularised by day 14 since there was no IP barrier present.

Histopathological analysis of cecum, peritoneum and adhesion tissue allowed to further evaluate the differences in formation of peritoneal adhesions in time between control and GP-MS-treated mice. Tissue samples of control mice clearly showed inflammation. Two days after induction of peritoneal adhesions (Suppl. Figure 2a), a limited to mild active inflammation of the cecal serosa was seen, while the cecal mucosa displayed a normal architecture. Peritoneal tissue also displayed mildly active inflammation. Adhesion tissue consisted of adipose tissue, infiltrated by neutrophils, and lymphoid follicles were occasionally observed. In comparison, in all cecal samples of GP-MS-treated mice, the serosa displayed limited inflammation as only few neutrophils and lymphocytes were present. Cecal mucosa did not display any abnormalities. Some neutrophils and lymphocytes were also noticed in peritoneal tissue, without infiltration into muscle tissue, indicating a mildly active inflammatory response.

Seven days after induction of peritoneal adhesions (Suppl. Figure 2b) extended inflammation of cecal serosa was observed in control mice. Both neutrophils and lymphocytes were noticed at the entire surface of the serosa. Peritonitis is clearly observed in control mice with extension of the inflammation into muscle tissue of abdominal wall. Adhesion tissue consisted of adipose tissue with inflammatory cells and lymphoid aggregates. Cecal serosa and mucosa of GP-MS-treated mice displayed no irregularities at day 7, whereas a small amount of inflammatory cells was observed in peritoneal tissue. No infiltration into muscle tissue of abdominal wall was seen.

Fourteen days after induction of peritoneal adhesions (Suppl. Figure 2c), adipose tissue associated with cecum of control mice, i.e. adhesion tissue, showed a severe inflammatory infiltrate. Cecal mucosa displayed normal architecture whereas serositis was observed. Peritoneal tissue still showed active inflammation after fourteen days. Inflammatory cells were observed in adipose, connective and muscle tissue. Chronic inflammation was seen upon observation of adhesion tissue. Cecal mucosa and serosa of GP-MS-treated mice had a normal appearance without signs of inflammation. Peritoneal tissue of most mice was healed after abrasion, although in some cases, a few

inflammatory cells were observed. None of the tissues showed penetration of inflammatory cells into abdominal wall muscle tissue. Thus, histopathological examination showed that inflammatory reaction of cecum and peritoneum decreased over time. Cecum and peritoneum recovered and displayed normal histological appearance. Quantification of inflammatory markers, cytokines in plasma and peritoneal fluid, is performed in the proof-of-concept study detailed below. This permits confirmation of the hypothesis that GP-MS are able to reduce formation of peritoneal adhesions and allow healing of peritoneal wounds.

3.5.2.2. Proof of concept: effectiveness of GP-MS in the prevention of postsurgical peritoneal adhesions in a standardized mouse model

All animals had a healthy appearance and their general activity was normal. Furthermore, they gained body weight after the surgical procedure. Adhesions were seen in all control mice and animals of the comparison group (Hyalobarrier®). In the intervention group (GP-MS treated mice) 36% of the mice developed at least one adhesion, which represented a statistic significant reduction of 64% in incidence compared to the control group (P=0.0039; Fisher's Exact). The high incidence (100%) of adhesions noticed in the control group indicates that the standardized adhesion model is adequate to evaluate the effectiveness of agents in the prevention of postsurgical peritoneal adhesions.

The results of the quantitative scoring of the peritoneal adhesions are displayed in Table 7. Visceral adhesions were seen in all animals of the control (Figure 10A) and Hyalobarrier® group (Figure 10D), compared to 18% of GP-MS treated mice (Figure 10F). The mice predominantly developed intestine-intestine adhesions. Parietal adhesions were seen in 64% and 45% of mice in the control (Figure 10B) and Hyalobarrier® group (Figure 10C), respectively. Parietal adhesions were observed in 18% of GP-MS treated animals. At day 14, adhesions were vascularized in 91% of mice in the control group compared to 9% of animals in the GP-MS group. Vascularized adhesions were observed in 82% of Hyalobarrier®-treated mice. It should be noted that when intestines are immediately attached to the peritoneal wall, observation of vascularization is not possible, hence there are no fibrous adhesion strands present.

Results of the qualitative assessment of peritoneal adhesions are displayed in Table 8. The total adhesion score of the control group was 7.90 ± 1.70 compared to 1.18 ± 1.78 in the GP-MS group. The difference in total score between both groups was statistically significant ($P < 0.0001$; Wilcoxon-Mann Whitney). In addition, the GP-MS group (1.18 ± 1.78) and Hyalobarrier® group (8.36 ± 1.91) differed significantly in total adhesion score ($P < 0.0001$; Wilcoxon-Mann Whitney), whereas no statistically significance was reported between Hyalobarrier® and control group (P=0.42; Wilcoxon-Mann Whitney).

Dense adhesions were observed in 82% and 91% of mice in the Hyalobarrier® and control group, respectively, whereas only filmy adhesions were seen in the GP-MS group. Furthermore, adhesions of GP-MS treated mice were very localized (extent of 0.45 ± 0.69) and felt easily apart. The 4 GP-MS-treated mice where adhesions were observed had only 1 or 2 filmy adhesions which did not lead to clinical relevant complication[58]. Extended adhesions where ± 70% of peritoneal cavity was involved, were observed in Hyalobarrier® (extent of 3.00 ± 1.10) and control group (extent of 2.64 ± 0.47). The adhesions mainly required sharp dissection to separate and was not possible without damaging of viscera of intestines or peritoneum.

An overview of the evaluation of the adhesion grading according to the Zühkle classification is displayed in Table 9. All control mice developed grade 3 (55%) or 4 (27%) peritoneal adhesions except for two (18%) mice, who had grade 2 adhesions. Hyalobarrier®-treated mice developed grade 3 (27%) or 4 (64%) peritoneal adhesions, except for one mouse (9%) with grade 2 adhesions. No adhesions (grade 0) were observed in 64% of GP-MS-treated mice and 36% developed grade 1 adhesions. Consequently, a significant lower grade of adhesion was seen in the GP-MS-treated mice (0.36 ± 0.50) compared to the control group (3.09 ± 0.70) and comparison group (3.55 ± 0.69), respectively ($P < 0.0001$; Wilcoxon-Mann Whitney). Control and Hyalobarrier® group did not differ statistically significant in grade of adhesion ($P=0.1432$; Wilcoxon-Mann Whitney).

It can be concluded that GP-MS are able to prevent formation of postsurgical adhesions since each scoring system, quantitative and qualitative scoring and grading of adhesions, demonstrates a statistic significant reduction in extent, type, tenacity or adhesion grade when compared to the control or Hyalobarrier® groups. Remarkably, Hyalobarrier® did not significantly reduce peritoneal adhesions. Hyalobarrier® gel was selected since it has a similar characteristics as GP-MS (mechanism of action, biodegradable, gel). Hyalobarrier® gel is a sterile, transparent and highly viscous gel, registered in Europe for open surgical procedures. Beside, Hyalobarrier® gel Endo is available in Europe, which is indicated for laparoscopic and hysteroscopic surgery. Hyalobarrier® gel is composed of 4% auto-crosslinked polysaccharide (ACP) in contrast to Hyalobarrier® Endo, a 3% ACP gel. The ACP polymers are obtained through an auto-crosslinking process that results in intra- and intermolecular condensation of hyaluronic acid[59]–[61]. Although Seprafilm®, Interceed® and Adept® are most commonly used in clinical practice[62], the effectiveness of GP-MP was compared to Hyalobarrier® gel. In contrast to Hyalobarrier® gel, Seprafilm® and Interceed® are absorbable solid devices, which are applied as a film on the injured surfaces. Adept® was not selected since it is a liquid barrier instead of a solid device and thereby attempts to separate injured surfaces by hydroflotation[1]. Additionally, Adept® shows a limited peritoneal retention, characteristic for liquid agents[4]. Despite several similarities between GP-MS and Hyalobarrier® gel, there is one major difference between both treatments. The GP-MS are intraperitoneally injected after complete closure of the ventral incision without attempt to direct the

formulation towards the traumatized areas whereas Hyalobarrier® gel is applied directly in a thin layer at the assumed sites of adhesion and stays in place due to its viscous and sticky properties.

Other studies reported that Hyalobarrier® was able to reduce adhesions. Binda et al. reported a significant reduction of adhesions in Balb/c mice, but the research methodology was different from this study since adhesions were laparoscopically induced by hypoxia and normoxia[59], [63], [64]. Efficacy of Hyalobarrier® was investigated in a rat uterine horn model[65], [66]. The effect of Hyalobarrier was not yet investigated in a standard abraded peritoneal wall-cecum model. This study does not demonstrate a significant reduction of adhesion when compared to saline and therefore its efficacy cannot be confirmed in this mouse model.

Histopathological examination of cecum, abdominal wall and, if applicable, adhesion tissue was performed. Generally, cecal serosa and mucosa of GP-MS-treated mice did not display irregularities (Suppl. Figure 3a). Visceral adhesions were observed in two GP-MS-treated mice, analysis of cecum confirmed mild serositis. Peritoneal tissue had a normal appearance. Local inflammation of mesothelium of two GP-MS-treated mice with parietal adhesions was noticed, but there was no infiltration into muscle tissue of abdominal wall. Adhesion tissue consisted of adipose tissue with lymphocytic infiltration. Cecal serositis was seen in all control mice with no abnormalities of cecal mucosa. Inflammatory cells were abundantly present when cecum was adhered to abdominal wall. All control mice showed peritonitis with extensive infiltration into muscle tissue of abdominal wall (Suppl. Figure 3b). Lymphocytes were observed in adipose tissue of adhesions. Analysis of cecum, peritoneum and adhesion tissue of Hyalobarrier-treated mice (Suppl. Figure 3c) showed similar characteristics of inflammation as tissues of control mice. In conclusion, histopathological examination confirmed the results of scoring of adhesions. GP-MS are able to prevent peritoneal adhesions and thereby recover normal histology of cecum and peritoneum. In contrast, mild to severe inflammation of cecal serosa and peritoneum was observed in all control and Hyalobarrier-treated mice.

Subsequently, cytokines IL-1ß, IL-6 and TNF-α, inflammatory markers released during the peritoneal adhesions cascade[1], [2], were analysed in plasma and peritoneal fluid. None of the cytokines were present in plasma above the limit of detection (55.2 pg/ml for IL-1ß, 58.8 pg/ml for IL 6, 30.5 pg/ml for TNF-α) at any time point (day 1, 7 and 14 post-operative). Cytokine analysis of peritoneal fluid (Suppl. Figure 4) illustrated that concentration of IL-1ß, IL-6 and TNF-α of control and Hyalobarrier-treated mice were slightly higher than GP-MS-treated mice at any time point but without significant difference. Cytokines were most abundantly present at day 1 after abrasion of cecum and peritoneum. IL-1 and TNF-α are produced by activated macrophages in peritoneal fluid and mainly important in the early phase of wound healing. Production of IL-6 is up-regulated by IL-1 and TNF-α. These cytokines interact with the fibrinolytic pathway and influence the remodeling of the extracellular matrix which may be responsible for formation of adhesions after peritoneal injury[67]. Concentration of

cytokines after induction of adhesions was higher for all animals than before induction. It has been reported that surgical tissue trauma is followed by a cascade of inflammatory signaling and activation of epithelial, endothelial and inflammatory cells, platelets and fibroblasts[68]. Nevertheless, no significant difference could be appointed and concentrations of cytokines were around limit of detection. The local induction of adhesions could be an explanation for the limited increase of concentration of cytokines, while a more extensive and aggressive model of induction of peritoneal adhesions could possibly induce a higher increase of cytokines in peritoneal fluid.

4. Conclusion

Spheroid gelatin microspheres were prepared by a modified emulsification solvent extraction method. Microspheres were stabilized by crosslinking using genipin. GP-MS did not influence cell viability when analysed by MTT assays using SKOV-3 cells. *In vivo* studies in mice showed excellent biocompatibility, distribution and degradation characteristics of GP-MS. GP-MS appear to be a promising strategy to prevent postoperative peritoneal adhesions. GP-MS-treated mice developed significantly less postsurgical adhesions when compared to saline and Hyalobarrier®-treated animals. Future work will include the incorporation of a cytostatic agent into the microspheres. Drug release will be monitored *in vitro* and *in vivo*. In addition, the potential efficacy of the drug-loaded microspheres will be evaluated in a mouse model for peritoneal metastasis of ovarian origin.

5. References

[1] T. Liakakos, N. Thomakos, P. M. Fine, C. Dervenis, and R. L. Young, "Peritoneal Adhesions : Etiology , Pathophysiology , and clinical significance," *Dig Surg*, vol. 14233, pp. 260–273, 2001.

[2] G. Pados, A. Makedos, and B. Tarlatzis, "Adhesion Prevention Strategies in Laparoscopic Surgery," 2013.

[3] W. Arung, M. Meurisse, and O. Detry, "Pathophysiology and prevention of postoperative peritoneal adhesions," *World J. Gastroenterol.*, vol. 17, no. 41, pp. 4545–4553, 2011.

[4] C. Brochhausen, V. H. Schmitt, C. N. E. Planck, T. K. Rajab, D. Hollemann, C. Tapprich, B. Krämer, C. Wallwiener, H. Hierlemann, R. Zehbe, H. Planck, and C. J. Kirkpatrick, "Current Strategies and Future Perspectives for Intraperitoneal Adhesion Prevention," *J. Gastrointest. Surg.*, vol. 16, no. 6, pp. 1256–1274, 2012.

[5] H. van Goor, "Consequences and complications of peritoneal adhesions," *Color. Dis.*, vol. 9, no. SUPPL. 2, pp. 25–34, 2007.

[6] X. Gao, X. Deng, X. Wei, H. Shi, F. Wang, T. Ye, B. Shao, W. Nie, Y. Li, M. Luo, C. Gong, and N. Huang, "Novel thermosensitive hydrogel for preventing formation of abdominal adhesions," *Int. J. Nanomedicine*, vol. 8, pp. 2453–2463, 2013.

[7] T. Ito, Y. Yeo, C. B. Highley, E. Bellas, C. a. Benitez, and D. S. Kohane, "The prevention of peritoneal adhesions by in situ cross-linking hydrogels of hyaluronic acid and cellulose derivatives," *Biomaterials*, vol. 28, no. 6, pp. 975–983, 2007.

[8] N. Bakrin, E. Cotte, F. Golfier, F. N. Gilly, G. Freyer, W. Helm, O. Glehen, and J. M. Bereder, "Cytoreductive Surgery and Hyperthermic Intraperitoneal Chemotherapy (HIPEC) for Persistent and Recurrent Advanced Ovarian Carcinoma: A Multicenter, Prospective Study of 246 Patients," *Ann. Surg. Oncol.*, no. July 2011, pp. 4052–4058, 2012.

[9] B. C., A. C., G. F.N., and G. O., "Treatment of peritoneal carcinomatosis in gastric cancers," *Dig. Dis.*, vol. 22, no. 4, pp. 366–373, 2004.

[10] D. L. Chan, D. L. Morris, A. Rao, and T. C. Chua, "Intraperitoneal chemotherapy in ovarian cancer: A review of tolerance and efficacy," *Cancer Manag. Res.*, vol. 4, no. 1, pp. 413–422, 2012.

[11] E. de Bree, a J. Witkamp, and F. a N. Zoetmulder, "Intraperitoneal chemotherapy for colorectal cancer.," *J. Surg. Oncol.*, vol. 79, no. 1, pp. 46–61, 2002.

[12] M.-K. Gervais, P. Dubé, Y. McConnell, P. Drolet, A. Mitchell, and L. Sideris, "Cytoreductive surgery plus hyperthermic intraperitoneal chemotherapy with oxaliplatin for peritoneal carcinomatosis arising from colorectal cancer.," *J. Surg. Oncol.*, vol. 108, no. 7, pp. 438–43, 2013.

[13] F. Mohamed, T. Cecil, B. Moran, and P. Sugarbaker, "A new standard of care for the management of peritoneal surface malignancy," *Curr. Oncol.*, vol. 18, no. 2, pp. 84–96, 2011.

[14] V. J. Verwaal, S. Bruin, H. Boot, G. van Slooten, and H. van Tinteren, "8-Year Follow-up of Randomized Trial: Cytoreduction and Hyperthermic Intraperitoneal Chemotherapy Versus

Systemic Chemotherapy in Patients with Peritoneal Carcinomatosis of Colorectal Cancer," *Ann. Surg. Oncol.*, vol. 15, no. 9, pp. 2426–2432, 2008.

[15] G. Bajaj and Y. Yeo, "Drug delivery systems for intraperitoneal therapy," *Pharm. Res.*, vol. 27, no. 5, pp. 735–738, 2010.

[16] L. De Smet, W. Ceelen, J. P. Remon, and C. Vervaet, "Optimization of drug delivery systems for intraperitoneal therapy to extend the residence time of the chemotherapeutic agent," *Sci. World J.*, vol. 2013, 2013.

[17] C. Gong, B. Yang, Z. Qian, X. Zhao, Q. Wu, X. Qi, Y. Wang, G. Guo, B. Kan, F. Luo, and Y. Wei, "Improving intraperitoneal chemotherapeutic effect and preventing postsurgical adhesions simultaneously with biodegradable micelles," *Nanomedicine Nanotechnology, Biol. Med.*, vol. 8, no. 6, pp. 963–973, 2012.

[18] Y. a. Domnina, Y. Yeo, J. Y. Tse, E. Bellas, and D. S. Kohane, "Spray-dried lipid-hyaluronan-polymethacrylate microparticles for drug delivery in the peritoneum," *J. Biomed. Mater. Res. - Part A*, vol. 87, no. 3, pp. 825–831, 2008.

[19] M. F. Flessner, "Intraperitoneal Drug Therapy : Physical and Biological Properties," in *Cancer treatment and research*, 2007, pp. 131–152.

[20] K. K. Kim and D. W. Pack, "Microspheres for Drug Delivery," *Biol. Biomed. Nanotechnol.*, pp. 19–50, 2006.

[21] S. Gunji, K. Obama, M. Matsui, Y. Tabata, and Y. Sakai, "A novel drug delivery system of intraperitoneal chemotherapy for peritoneal carcinomatosis using gelatin microspheres incorporating cisplatin," *Surg. (United States)*, vol. 154, no. 5, pp. 991–999, 2013.

[22] R. T. Liggins, S. D'Amours, J. S. Demetrick, L. S. MacHan, and H. M. Burt, "Paclitaxel loaded poly(L-lactic acid) microspheres for the prevention of intraperitoneal carcinomatosis after a surgical repair and tumor cell spill," *Biomaterials*, vol. 21, no. 19, pp. 1959–1969, 2000.

[23] M. Tsai, Z. Lu, M. G. Wientjes, and J. L. S. Au, "Paclitaxel-loaded polymeric microparticles: Quantitative relationships between in vitro drug release rate and in vivo pharmacodynamics," *J. Control. Release*, vol. 172, no. 3, pp. 737–744, 2013.

[24] D. S. Kohane, J. Y. Tse, Y. Yeo, R. Padera, M. Shubina, and R. Langer, "Biodegradable polymeric microspheres and nanospheres for drug delivery in the peritoneum," *J. Biomed. Mater. Res. - Part A*, vol. 77, no. 2, pp. 351–361, 2006.

[25] S. E. Mutsaers and S. Wilkosz, "Structure and function of mesothelial cells.," in *Cancer treatment and research*, vol. 134, 2007, pp. 1–19.

[26] E. Esposito, R. Cortesi, and C. Nastruzzi, "Gelatin microspheres: Influence of preparation parameters and thermal treatment on chemico-physical and biopharmaceutical properties," *Biomaterials*, vol. 17, no. 20, pp. 2009–2020, 1996.

[27] H.-C. Liang, W.-H. Chang, K.-J. Lin, and H.-W. Sung, "Genipin-crosslinked gelatin microspheres as a drug carrier for intramuscular administration: in vitro and in vivo studies.," *J. Biomed. Mater. Res. A*, vol. 65, no. 2, pp. 271–282, 2003.

[28] N. Adhirajan, N. Shanmugasundaram, and M. Babu, “Gelatin microspheres cross-linked with EDC as a drug delivery system for doxycyline: development and characterization.,” *J. Microencapsul.*, vol. 24, no. 7, pp. 647–659, 2007.

[29] L. Solorio, C. Zwolinski, A. W. Lund, M. J. Farrell, and P. Jan, “Gelatin microspheres crosslinked with genipin for local delivery of growth factors,” *J. Tissue Eng. Regen. Med.*, vol. 4, no. 7, pp. 514–523, 2011.

[30] M. a Vandelli, F. Rivasi, P. Guerra, F. Forni, and R. Arletti, “Gelatin microspheres crosslinked with D , L -glyceraldehyde as a potential drug delivery system : preparation , characterisation , in vitro and in vivo studies,” *Int. J. Pharm.*, vol. 215, pp. 175– 184, 2001.

[31] H. C. Liang, W. H. Chang, H. F. Liang, M. H. Lee, and H. W. Sung, “Crosslinking structures of gelatin hydrogels crosslinked with genipin or a water-soluble carbodiimide,” *J. Appl. Polym. Sci.*, vol. 91, no. August, pp. 4017–4026, 2004.

[32] L. P. Yan, Y. J. Wang, L. Ren, G. Wu, S. G. Caridade, J. B. Fan, L. Y. Wang, P. H. Ji, J. M. Oliveira, J. T. Oliveira, J. F. Mano, and R. L. Reis, “Genipin-cross-linked collagen/chitosan biomimetic scaffolds for articular cartilage tissue engineering applications,” *J. Biomed. Mater. Res. - Part A*, vol. 95 A, no. 2, pp. 465–475, 2010.

[33] H. J. Wei, H. H. Yang, C. H. Chen, W. W. Lin, S. C. Chen, P. H. Lai, Y. Chang, and H. W. Sung, “Gelatin microspheres encapsulated with a nonpeptide angiogenic agent, ginsenoside Rg1, for intramyocardial injection in a rat model with infarcted myocardium,” *J. Control. Release*, vol. 120, no. 1–2, pp. 27–34, 2007.

[34] G. Thakur, A. Mitra, D. Rousseau, A. Basak, S. Sarkar, and K. Pal, “Crosslinking of gelatin-based drug carriers by genipin induces changes in drug kinetic profiles in vitro,” *J. Mater. Sci. Mater. Med.*, vol. 22, no. 1, pp. 115–123, 2011.

[35] Y. Yuan, B. M. Chesnutt, G. Utturkar, W. O. Haggard, Y. Yang, J. L. Ong, and J. D. Bumgardner, “The effect of cross-linking of chitosan microspheres with genipin on protein release,” *Carbohydr. Polym.*, vol. 68, no. 3, pp. 561–567, 2007.

[36] Y. Zhang, Y. Fu, S. Zhou, L. Kang, and C. Li, “A straightforward ninhydrin-based method for collagenase activity and inhibitor screening of collagenase using spectrophotometry,” *Anal. Biochem.*, vol. 437, no. 1, pp. 46–48, 2013.

[37] D. M. Kirchmajer, C. a. Watson, M. Ranson, and M. in Het Panhuis, “Gelapin, a degradable genipin cross-linked gelatin hydrogel,” *RSC Adv.*, vol. 3, no. 4, p. 1073, 2013.

[38] A. H. MacIver, M. D. McCall, R. L. Edgar, A. L. Thiesen, D. L. Bigam, T. a. Churchill, and a. M. J. Shapiro, “Sirolimus drug-eluting, hydrogel-impregnated polypropylene mesh reduces intra-abdominal adhesion formation in a mouse model,” *Surgery*, vol. 150, no. 5, pp. 907–915, 2011.

[39] B. Yang, C. Gong, Z. Qian, X. Zhao, Z. Li, X. Qi, S. Zhou, Q. Zhong, F. Luo, and Y. Wei, “Prevention of post-surgical abdominal adhesions by a novel biodegradable thermosensitive PECE hydrogel.,” *BMC Biotechnol.*, vol. 10, p. 65, 2010.

[40] M. M. Binda, C. R. Molinas, a Bastidas, and P. R. Koninckx, “Effect of reactive oxygen species scavengers, antiinflammatory drugs, and calcium-channel blockers on carbon dioxide pneumoperitoneum-enhanced adhesions in a laparoscopic mouse model,” *Surg Endosc*, vol. 21, no. 10, pp. 1826–1834, 2007.

[41] F. Panahi, S. H. Sadraie, H. Khoshmohabat, E. Shahram, G. Kaka, and M. Hosseinalipour, "Macroscopic and pathological assessment of methylene blue and normal saline on postoperative adhesion formation in a rat cecum model," *Int. J. Surg.*, vol. 10, no. 9, pp. 537–541, 2012.

[42] M. Egea, A. Albasini, Z. Carmona, and P. Paricio, "Adhesion Response to Different Forms of Treating a Peritoneal Lesion: An Experimental Study in Rats," *Dig. Surg.*, vol. 12, no. 6, pp. 334–337, Jul. 1995.

[43] H. V Zühlke, E. M. Lorenz, E. M. Straub, and V. Savvas, "[Pathophysiology and classification of adhesions].," *Langenbecks Arch. Chir. Suppl. II. Verh. Dtsch. Ges. Chir.*, pp. 1009–16, Jan. 1990.

[44] X. Zhang, X. Chen, T. Yang, N. Zhang, L. Dong, S. Ma, X. Liu, M. Zhou, and B. Li, "The effects of different crossing-linking conditions of genipin on type I collagen scaffolds: an in vitro evaluation," *Cell Tissue Bank.*, vol. 15, no. 4, pp. 531–541, 2014.

[45] S. Fujikawa, Y. Fukui, K. Koga, T. Iwashita, H. Komura, and K. Nomoto, "Structure of genipocyanin G1, a spontaneous reaction product between genipin and glycine," *Tetrahedron Lett.*, vol. 28, no. 40, pp. 4699–4700, 1987.

[46] C. E. Brinckerhoff, J. L. Rutter, and U. Benbow, "Interstitial Collagenases as Markers of Tumor Progression Interstitial Collagenases as Markers of Tumor Progression 1," vol. 6, no. December, pp. 4823–4830, 2000.

[47] L. a Liotta and W. G. Stetler-Stevenson, "Tumor invasion and metastasis: an imbalance of positive and negative regulation.," *Cancer Res.*, vol. 51, no. 18 Suppl, p. 5054s–5059s, 1991.

[48] L. Herszényi, L. Barabás, I. Hritz, G. István, and Z. Tulassay, "Impact of proteolytic enzymes in colorectal cancer development and progression," vol. 20, no. 37, pp. 13246–13257, 2014.

[49] S. Rakash, "Role of proteases in cancer: A review," *Biotechnol. Mol. Biol. Rev.*, vol. 7, no. 4, pp. 90–101, 2012.

[50] S. Blockhuys, B. Vanhoecke, J. Smet, B. De Paepe, R. Van Coster, M. Bracke, and C. De Wagter, "Unraveling the mechanisms behind the enhanced MTT conversion by irradiated breast cancer cells.," *Radiat. Res.*, vol. 179, no. 4, pp. 433–43, 2013.

[51] M. Bracke, M.E., Depypere, H., Labit, C., Van Marck, V., Vennekens, K., Vermeulen, S.J., Maelfait, I., Philippé, J., Serreyn, R. and Mareel, "Functional downregulation of the E-cadherin/catenin complex leads to loss of contact inhibition of motility and of mitochondrial activity, but not of growth in confluent epithelial cell cultures," *Eur. J. Cell Biol.*, vol. 74, pp. 342–349, 1997.

[52] A. Bricou, R. E. Batt, and C. Chapron, "Peritoneal fluid flow influences anatomical distribution of endometriotic lesions: Why Sampson seems to be right," *Eur. J. Obstet. Gynecol. Reprod. Biol.*, vol. 138, no. 2, pp. 127–134, 2008.

[53] A. D. Levy, J. C. Shaw, and L. H. Sobin, "Secondary tumors and tumorlike lesions of the peritoneal cavity: imaging features with pathologic correlation.," *Radiographics*, vol. 29, no. 2, pp. 347–373, 2009.

[54] Y. Yeo, T. Ito, E. Bellas, C. B. Highley, R. Marini, and D. S. Kohane, “In situ cross-linkable hyaluronan hydrogels containing polymeric nanoparticles for preventing postsurgical adhesions.,” *Ann. Surg.*, vol. 245, no. 5, pp. 819–824, 2007.

[55] a H. Mohammadpour, a Tavassoli, M. R. Khakzad, E. Zibaee, M. Afshar, M. Hashemzaei, and G. Karimi, “Effect of gold nanoparticles on postoperative peritoneal adhesions in rats,” *Nanomed. J*, vol. 2, no. 23, pp. 211–216, 2015.

[56] M. Berkkanoglu, L. Zhang, M. Ulukus, H. Cakmak, U. a. Kayisli, S. Kursun, and A. Arici, “Inhibition of chemokines prevents intraperitoneal adhesions in mice,” *Hum. Reprod.*, vol. 20, no. 11, pp. 3047–3052, 2005.

[57] J. K. Jackson, K. C. Skinner, L. Burgess, T. Sun, W. L. Hunter, and H. M. Burt, “Paclitaxel-loaded crosslinked hyaluronic acid films for the prevention of postsurgical adhesions,” *Pharm. Res.*, vol. 19, no. 4, pp. 411–417, 2002.

[58] K. Falk, B. Lindman, S. Bengmark, K. Larsson, and L. Holmdahl, “Prevention of adhesions by surfactants and cellulose derivatives in mice.,” *Eur. J. Surg.*, vol. 167, no. 2, pp. 136–41, 2001.

[59] M. M. Binda and P. R. Koninckx, “Prevention of adhesion formation in a laparoscopic mouse model should combine local treatment with peritoneal cavity conditioning.,” *Hum. Reprod.*, vol. 24, no. 6, pp. 1473–9, 2009.

[60] R. L. DeWilde and G. Trew, “Postoperative abdominal adhesions and their prevention in gynaecological surgery. Expert consensus position. Part 2 - Steps to reduce adhesions,” *Gynecol. Surg.*, vol. 4, no. 4, pp. 243–253, 2007.

[61] V. Mais, G. L. Bracco, P. Litta, T. Gargiulo, and G. B. Melis, “Reduction of postoperative adhesions with an auto-crosslinked hyaluronan gel in gynaecological laparoscopic surgery: a blinded, controlled, randomized, multicentre study,” *Hum Reprod*, vol. 21, no. 5, pp. 1248–1254, 2006.

[62] T. K. Rajab, K. O. Kimonis, E. Ali, A. C. Offodile, M. Brady, and R. Bleday, “Practical implications of postoperative adhesions for preoperative consent and operative technique,” *Int. J. Surg.*, vol. 11, no. 9, pp. 753–756, 2013.

[63] M. M. Binda and P. R. Koninckx, “Hyperoxia and prevention of adhesion formation: a laparoscopic mouse model for open surgery.,” *BJOG*, vol. 117, no. 3, pp. 331–9, 2010.

[64] M. M. Binda, C. R. Molinas, A. Bastidas, M. Jansen, and P. R. Koninckx, “Efficacy of barriers and hypoxia-inducible factor inhibitors to prevent CO(2) pneumoperitoneum-enhanced adhesions in a laparoscopic mouse model.,” *J. Minim. Invasive Gynecol.*, vol. 14, no. 5, pp. 591–9, 2007.

[65] C. Kaya, N. Sever, H. Cengiz, Ş. Yıldız, M. Ekin, and L. Yaşar, “A randomized controlled study of the efficacy of misoprostol and hyaluronic acid in preventing adhesion formation after gynecological surgery: a rat uterine horn model.,” *Eur. J. Obstet. Gynecol. Reprod. Biol.*, vol. 176, pp. 44–9, 2014.

[66] M. Wallwiener, S. Brucker, H. Hierlemann, C. Brochhausen, E. Solomayer, and C. Wallwiener, “Innovative barriers for peritoneal adhesion prevention: liquid or solid? A rat uterine horn model,” *Fertil. Steril.*, vol. 86, no. 4 SUPPL., pp. 1266–1276, 2006.

[67] Y. C. Cheong, S. M. Laird, J. B. Shelton, W. L. Ledger, T. C. Li, and I. D. Cooke, “The correlation of adhesions and peritoneal fluid cytokine concentrations: a pilot study.,” *Hum. Reprod.*, vol. 17, no. 4, pp. 1039–1045, 2002.

[68] W. P. Ceelen and M. E. Bracke, “Peritoneal minimal residual disease in colorectal cancer: mechanisms, prevention, and treatment,” *Lancet Oncol.*, vol. 10, no. 1, pp. 72–79, 2009.

Figures

Figure 1: Hypothetic subdivision of the abdominal cavity[41].

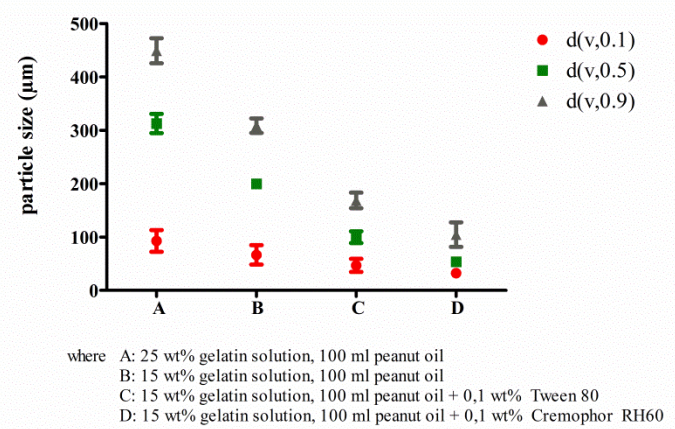

Figure 2: Influence of the composition of the emulsion on the size of the gelatin microspheres (n=3; ± SD)

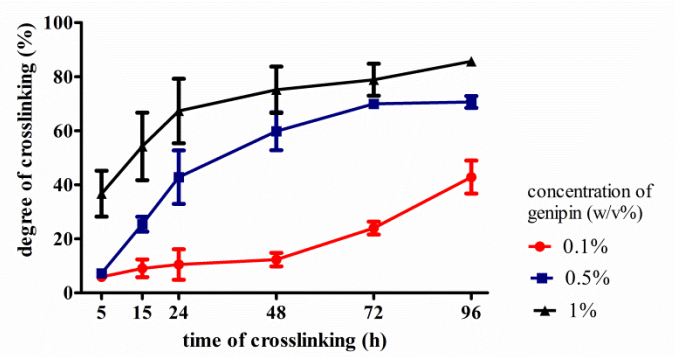

Figure 3: Degree of crosslinking (%) of gelatin microspheres (n=3; ± SD) in function of genipin concentration (0.1, 0.5 1 w/v% genipin) and crosslinking time (h)

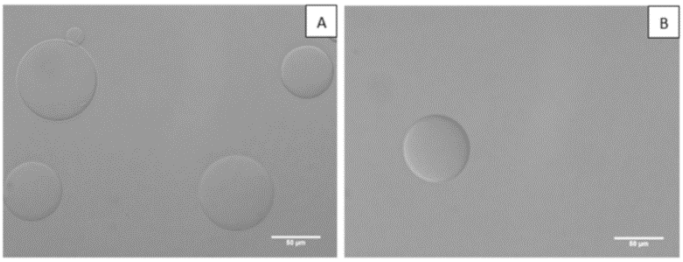

Figure 4: **Photomicrographs of genipin-crosslinked gelatin microspheres after (a) 5h and (b) 24 h of crosslinking using 0.5 w/v % genipin**

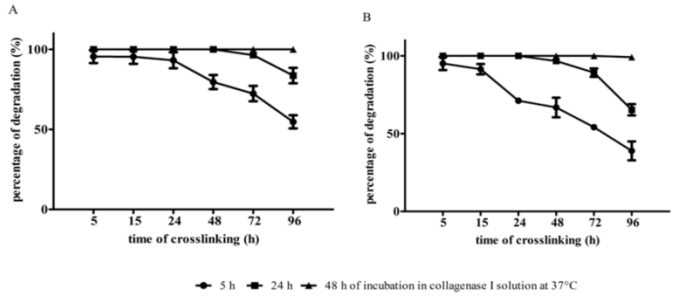

Figure 5: In vitro enzymatic (collagenase I) degradation of gelatin microspheres (n=3; ±SD) crosslinked using 0.1 w/v % (A) and 0.5 w/v % (B) genipin and different crosslinking times

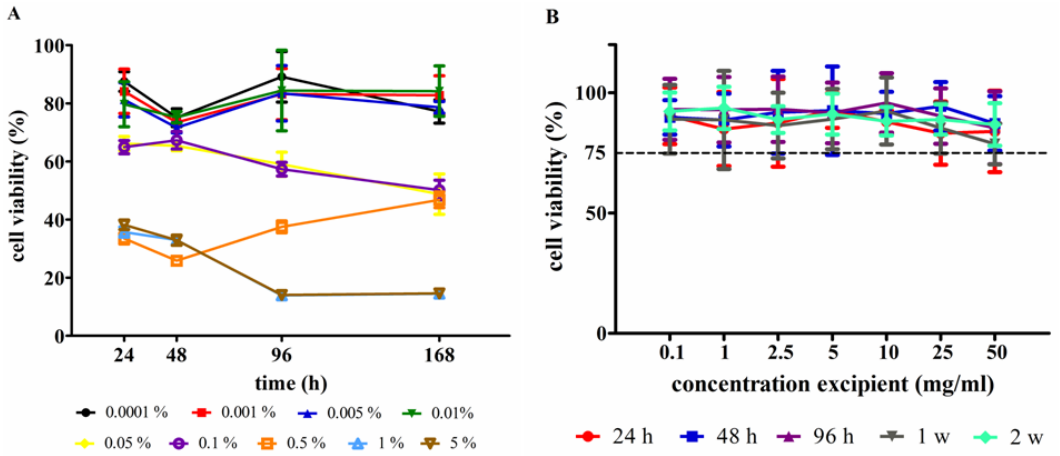

Figure 6: (A) influence of genipin concentration (% w/v) in the reaction medium on cell viability in time measured by MTT assay on SKOV-3 cells (n= 18, ± SD); (B) influence of concentration of GP-MS on cell viability of SKOV-3 cells in time (n=18, ± SD)

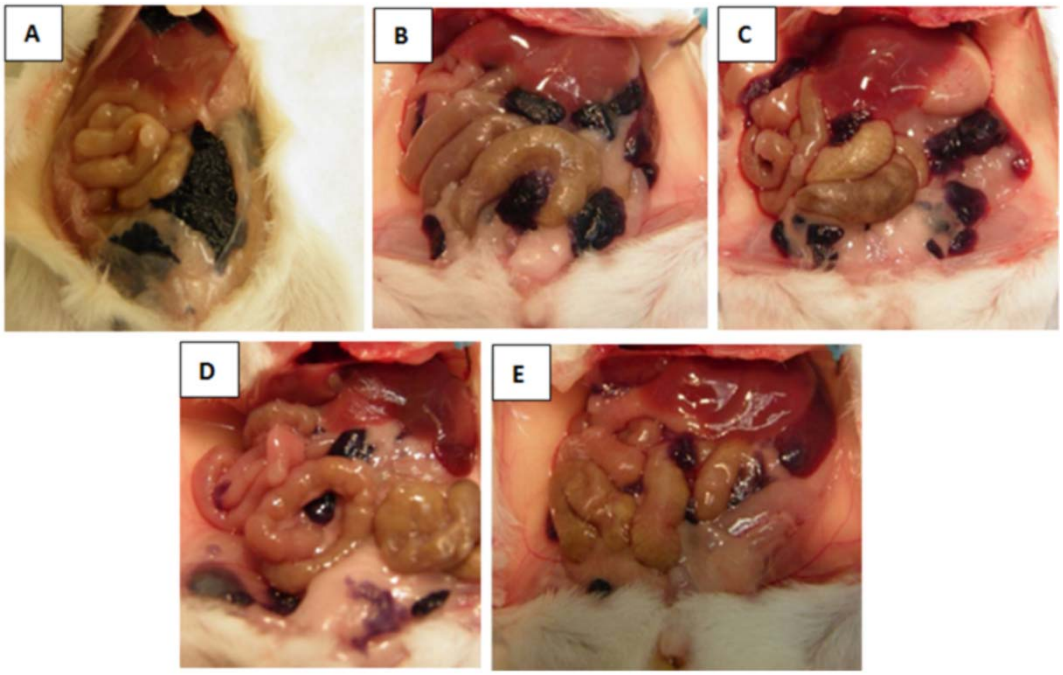

Figure 7: macroscopic images of abdominal cavity of Balb/c mice. Evaluation of distribution pattern of GP-MS 2 days (A), 7 days (B), 14 days (C), 21 days (D) and 28 days (E) after IP injection.

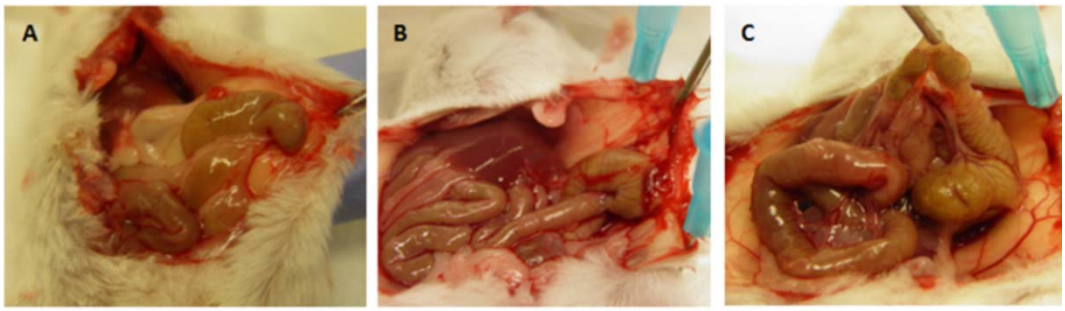

Figure 8 : Photographs of the abdominal cavity of control mice after induction of peritoneal adhesions (A) Day 2: type 3 adhesions, qualitative score of 8 (B) Day 7: type 3 adhesions, qualitative score of 8 (C) Day 14: type 3 adhesions, qualitative score of 9 (vascularised)

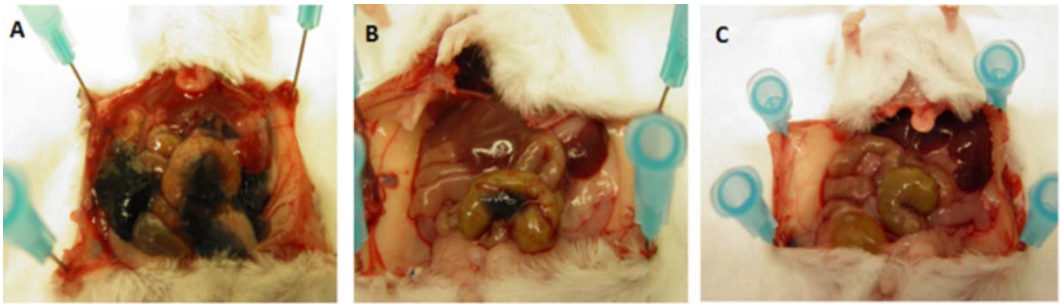

Figure 9: Photographs of the abdominal cavity of GP-MS-treated mice after induction of peritoneal adhesions (A) Day 2: no adhesions, (B) Day 7: formulation almost completely degraded, no adhesions (C) Day 14: formulation entirely degraded, no adhesions

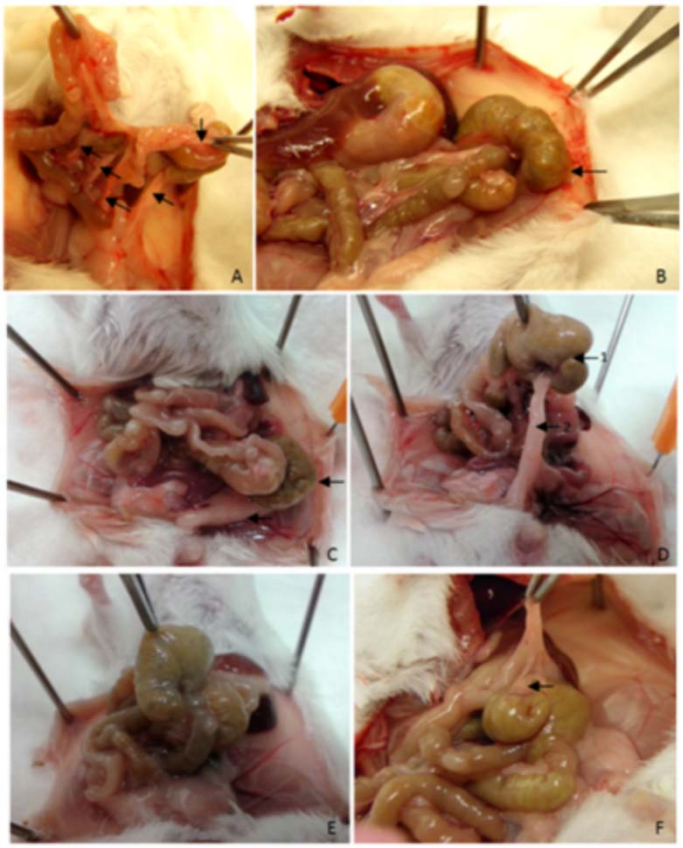

Figure 10: Photographs of the abdominal cavity 14 days after induction of peritoneal adhesions. Control mouse: (A) visceral adhesions, (B) parietal adhesion, colon attached to peritoneum; Hyalobarrier®-treated mouse: (C) parietal adhesions, cecum attached to peritoneum, (D) 1=visceral adhesion, 2=parietal adhesion, cecum attached together; GP-MS-treated mouse: (E) no adhesions, normal physiology, (F) filmy adhesion between cecum and greater omentum. Arrows indicate peritoneal adhesions.

Tables

Table 1: Qualitative adhesion scoring system[40]

Category	Score
Extent	
No adhesion	0
1-25% of the peritoneal cavity involved	1
26-50% of the peritoneal cavity involved	2
51-75% of the peritoneal cavity involved	3
76-100% of the peritoneal cavity involved	4
Type	
No adhesion	0
Filmy	1
Dense	2
Vascular	3
Tenacity	
No adhesion	0
Easily fall apart	1
Require traction	2
Require sharp dissection	3
Total adhesion score (Extent + Type + Tenacity)	0-10

Table 2: Quantitative adhesion scoring system[42]

Criteria	
Site of adhesions	
Parietal	Pelvic fat body-abdominal wall Omentum-abdominal wall Intestine-abdominal wall
Visceral	Omentum-liver/stomach Intestine-intestine Liver-stomach
Tenacity	
Type 0	No adhesion
Type I	Simple, without dissection
Type II	Dissection needed to separate adherent area
Type III	Dissection needed to cut the adhesions
Vascularization of adhesions	
Vascularized Avascularized	

Table 3: The Zühlke grading classification of adhesions[43]

Grade	Description
Grade 0	No adhesion
Grade I	Filmy adhesions that require gently blunt dissection to be divided
Grade II	Mild adhesions that require aggressive blunt dissection to be freed
Grade III	Moderate adhesions that require sharp dissection to be freed
Grade IV	Severe adhesions that are not dissectible without damage to adherent organs

Table 4: Influence of surfactants on the size of gelatin microspheres (n=3)

Surfactant	D[4,3] ± SD (µm) (n=3)
sorbitan esters (Span®) and their ethoxylates (Tween®)	
Tween® 20	147 ± 13
Tween® 80	84 ± 13
Tween® 80/Span® 80	71 ± 4
Tween® 85	119 ± 29
Span® 85/Tween® 85	110 ± 12
poloxamers (Pluronic®)	
Pluronic® F68	155± 23
Pluronic® F127	270 ± 15
Pluronic® L121	65 ± 11
polyethoxylated castor oil (Cremophor® RH)	
Cremophor® RH 60	58 ± 10

Table 5: Degradation time (d) of genipin-crosslinked microspheres (n=3; ±SD) by hydrolysis at 37 °C

Crosslinking time (h)	5	15	24	48	72	96
% w/v genipin	time needed to degrade the microspheres (d)					
0.1	1.0 ± 0.0	1.0 ± 0.0	2.7 ± 0.6	3.7 ± 0.6	4.3 ± 0.6	8.3 ± 0.6
0.5	2.0 ± 0.0	7.3 ± 0.6	17.0 ± 1.0	29.0 ± 1.0	37.0 ± 2.0	41.7 ± 2.5
1.0	4.0 ± 1.0	15.7 ± 1.5	43.3 ± 1.5	51.3 ± 0.6	53.7 ± 1.2	58.7 ± 2.1

Table 6 : Qualitative and quantitative valuation of peritoneal adhesions in GP-MS-treated (n=12; 3 per time point) and control mice (n=3; 1 per time point) on post-operative day 2, 7 and 14.

Post-operative day	Quality of adhesions		Quantity of adhesions	
	GP-MS treated mice	Control mice	GP-MS treated mice	Control mice
	Total score		Tenacity (Type)	
Day 2	0	8	0	3
Day 7	0	8	0	3
Day 14	0	9	0	3

Table 7: Quantitative scoring of adhesions per treatment group (control, Hyalobarrier® and GP-MS group) including site of adhesions, tenacity and vascularization.

Category	Control (n=11)	Hyalobarrier® (n=11)	GP-MS (n=11)
Site adhesions			
Parietal	7	5	2
Visceral	11	11	2
Tenacity			
Type 0	0	0	7
Type I	0	0	4
Type II	5	3	0
Type III	6	8	0
Vascularization	10	9	1

Table 8: Qualitative scoring of peritoneal adhesions post-operative day 14. Results are displayed as average score ± standard deviation per category for each treatment group (n=11).

Category	Control group (n=11)	Hyalobarrier® group (n=11)	GP-MS group (n=11)
Extent	2.64 ± 0.92	3.00 ± 1.10	0.45 ± 0.69
Type	2.55 ± 0.69	2.64 ± 0.47	0.27 ± 0.47
Tenacity	2.73 ± 0.47	2.73 ± 0.47	0.45 ± 0.69
Total score	7.91 ± 1.70	8.36 ± 1.91	1.18 ± 1.78

Table 9: Number of mice and total average grade ± SD per adhesion grade according to the Zühkle classification per treatment group.

Grade	Control group (n=11)	Hyalobarrier® group (n=11)	GP-MS group (n=11)
Grade 0	0	0	7
Grade I	0	0	4
Grade II	2	1	0
Grade III	6	3	0
Grade IV	3	7	0
Average	3.09 ± 0.70	3.55 ± 0.69	0.36 ± 0.50

Supplementary data

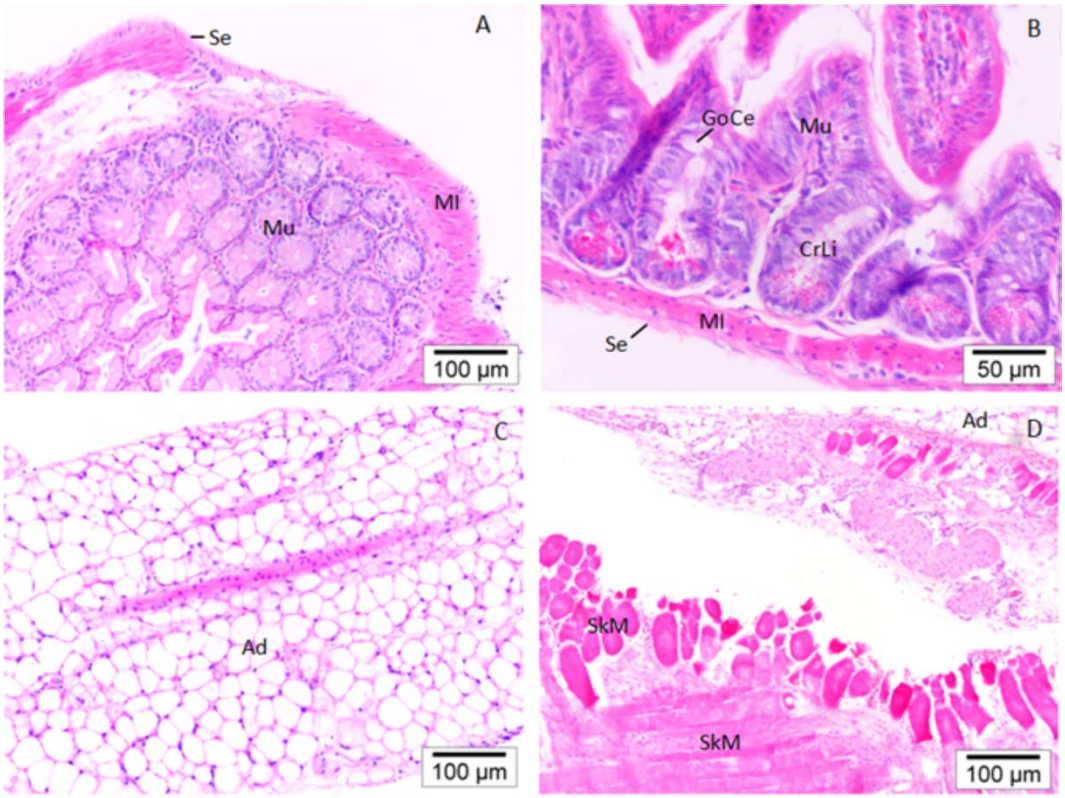

Figure 1a: Optical micrographs of H&E-stained slices of tissues of GP-MS-treated mice. (A) cecum, where MI = muscularis, Mu = mucosa, Se = serosa; (B) colon, where CrLi = Crypt of Lieberkühn, GoCe= Goblet Cell, MI = muscularis, Mu = mucosa, Se = serosa; (C) Greater Omentum, where A=Adipose Tissue; (D) Peritoneum/Abdominal Wall, where Ad=Adipose Tissue, SkM= Skeletal Muscle. Original magnification of 200x (A, C, D) and 400x (B).

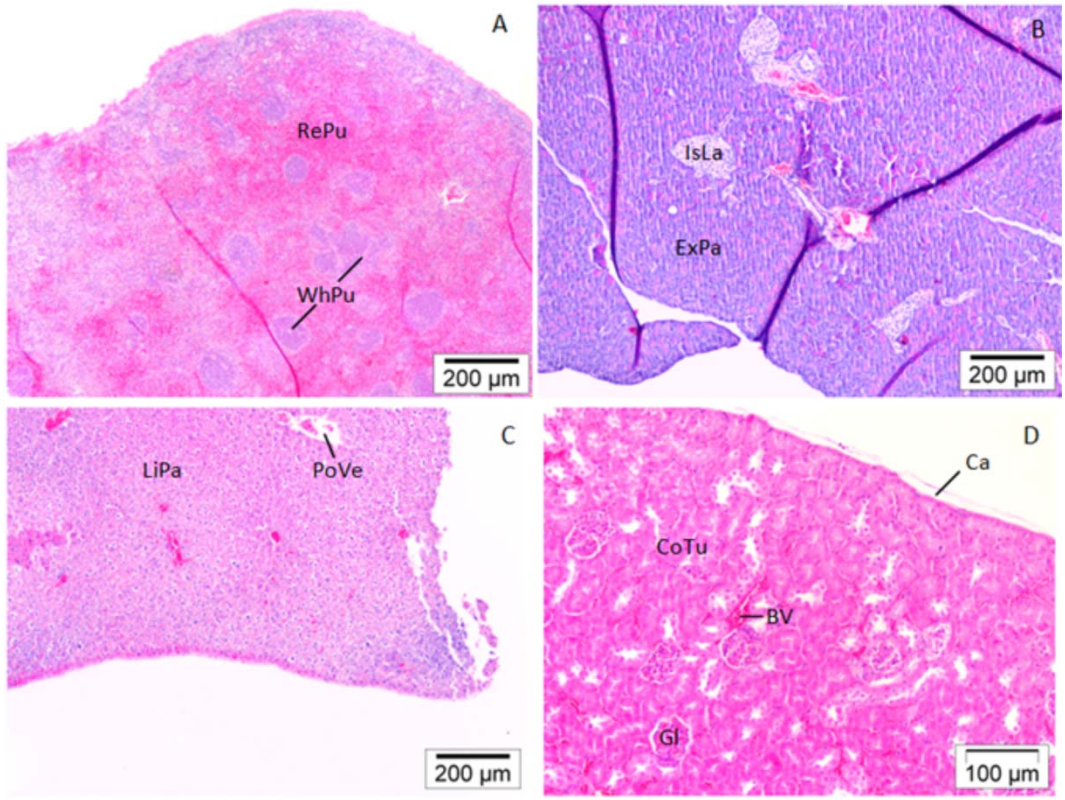

Figure 1b: Optical micrographs of H&E-stained slices of tissues of GP-MS-treated mice. (A) Spleen, where RePu = Red Pulp, WhPu = White Pulp; (B) Pancreas, where ExPa = Exocrine Pancreas, IsLa = Islet of Langerhans; (C) Liver, where LiPa = Liver Parenchyma, PoVe = Portal Vein; (D) Kidneys, where BV = Blood Vessel, Ca = Capsule, CoTu = Convoluted Tubule, Gl = Glomerulus . Original magnification of 100x (A,B,C) and 200x (D).

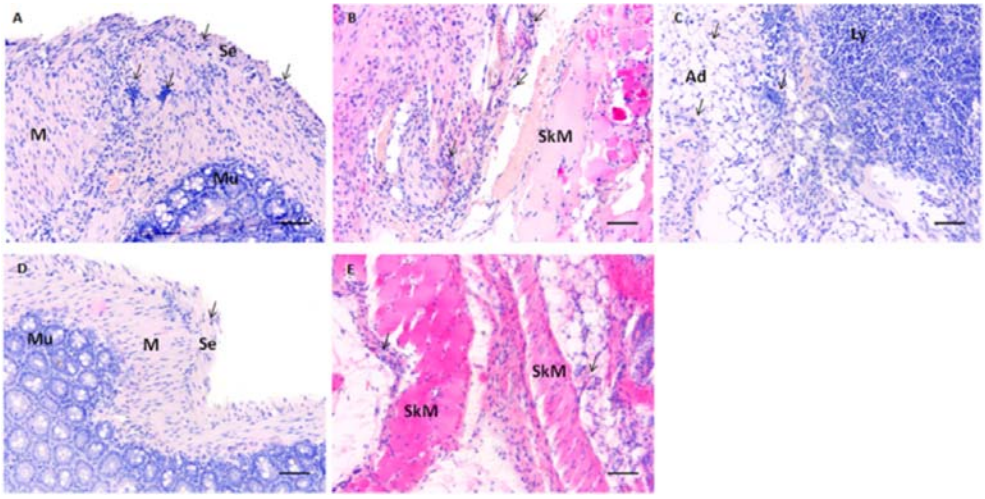

Figure 2a: Optical micrographs of H&E-stained slices of tissues of mice two days after induction of peritoneal adhesions. Inflammatory cells are observed in cecum (A), abdominal wall/peritoneum (B) and adhesion (C) of control mice. Cecum (D) and abdominal wall/peritoneum (E) of GP-MS-treated mice also displayed inflammatory cells. Scale bar represents 100 µm. Original magnification of 200x. Ad = adipose tissue, Ly = lymph node, M = muscularis, Mu = mucosa, Se = serosa, SkM = skeletal muscle, arrows indicate inflammatory cells.

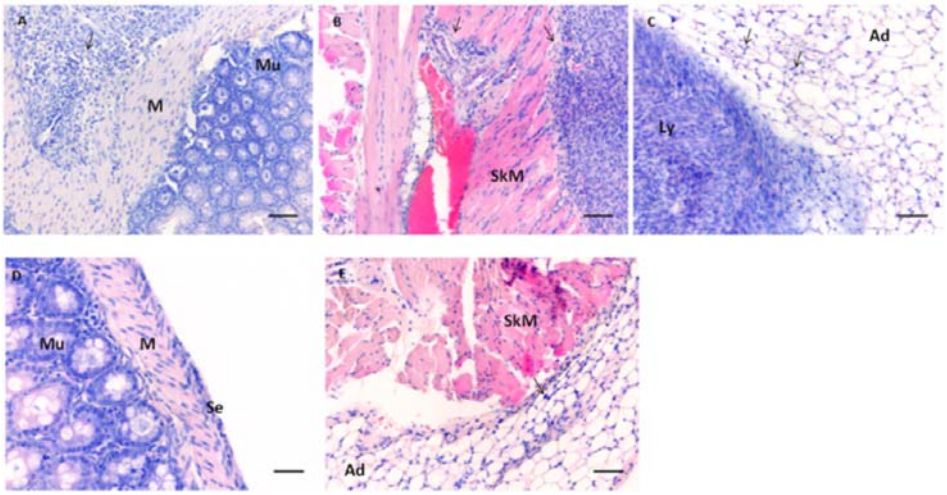

Figure 2b: Optical micrographs of H&E-stained slices of tissues of mice seven days after induction of peritoneal adhesions. Inflammatory cells are observed in cecum (A), abdominal wall/peritoneum (B) and adhesion (C) of control mice. Cecum of GP-MS-treated mice (D) displays normal architecture and few inflammatory cells are seen at abdominal wall/peritoneum (E) of GP-MS-treated mice. Scale bar represents 100 µm (A-C and E) or 50 µm (D). Original magnification of 200x (A-C and E) and 400x (D). Ad = adipose tissue, Ly = lymph node, M = muscularis, Mu = mucosa, Se = serosa, SkM = skeletal muscle, arrows indicate inflammatory cells.

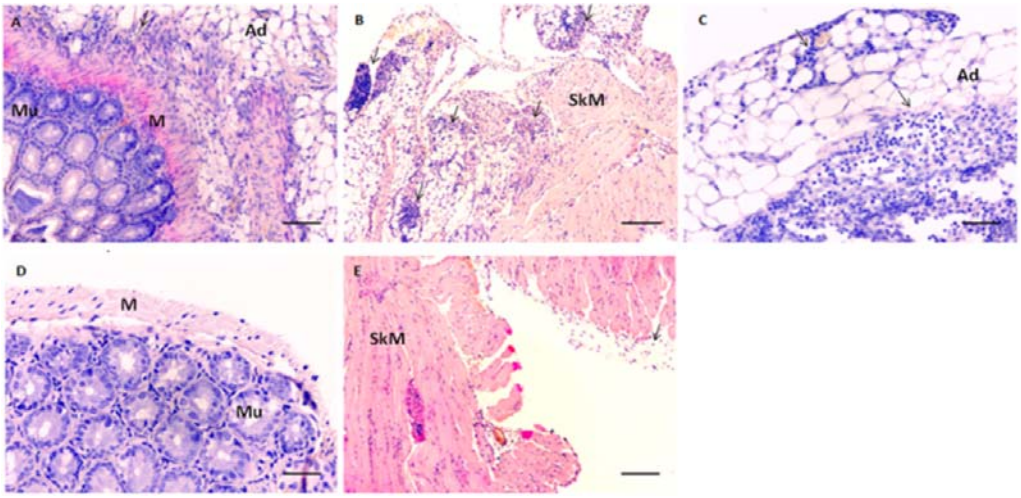

Figure 2c: Optical micrographs of H&E-stained slices of tissues of mice fourteen days after induction of peritoneal adhesions. Extensive inflammation is observed in cecum (A), abdominal wall/peritoneum (B) and adhesion (C) of control mice. Cecum of GP-MS-treated mice (D) displays normal architecture and few inflammatory cells are seen at abdominal wall/peritoneum (E) of GP-MS-treated mice. Scale bar represents 100 µm (A-C and E) or 50 µm (D). Original magnification of 200x (A-C and E) and 400x (D). Ad = adipose tissue, M = muscularis, Mu = mucosa, SkM = skeletal muscle, arrows indicate inflammatory cells

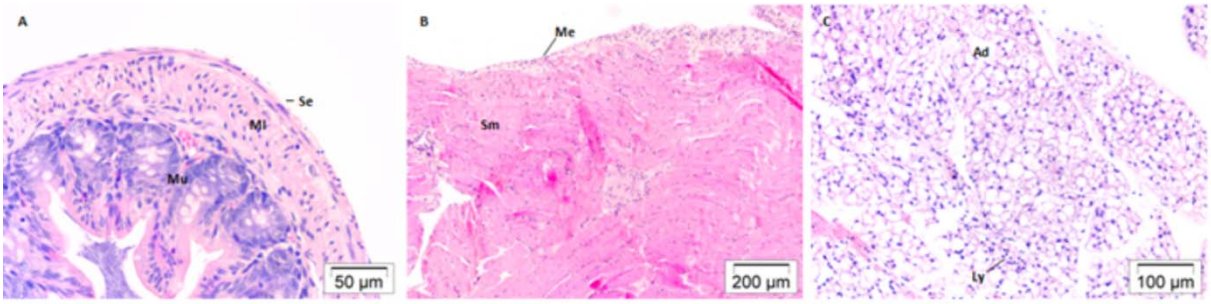

Figure 3a: Optical micrographs of H&E-stained slices of tissues of GP-MS-treated mice two weeks after induction of peritoneal adhesions. Cecum (A) and peritoneum/abdominall wall (B) display normal architecture. Adhesion tissue (C) consists of adipose tissue with inflammatory cells. Original magnification of 400x (A), 200x (B), 100x (C). Ad = adipose tissue, Ly = lymphocytes, Me = mesothelium, MI = muscularis, Mu = mucosa, Se = serosa, Sm = smooth muscle.

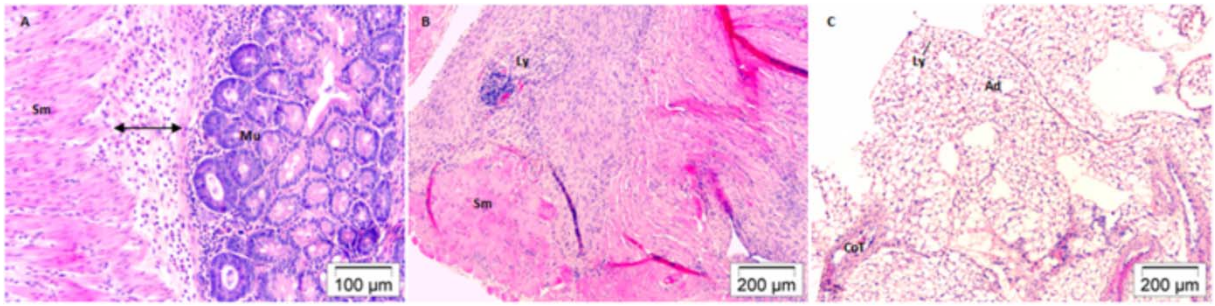

Figure 3b: Optical micrographs of H&E-stained slices of tissues of control mice two weeks after induction of peritoneal adhesions. (A) adhesion formed between abdominal wall and cecum. Arrow indicates inflammatory infiltrate. Original magnification of 200x. (B) Massive infiltration of inflammatory cells into mesothelium and smooth muscle. (C) Adhesion tissue consisting of adipose cells, connective tissue and inflammatory cells. Original magnification of 100x (B and C). Ad = adipose tissue, CoT = connective tissue, Ly = lymphocytes, Mu = mucosa, Sm = smooth muscle.

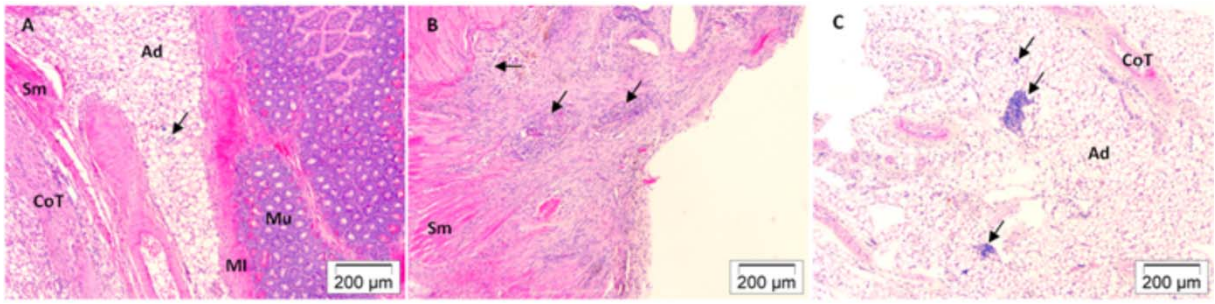

Figure 3c: Optical micrographs of H&E-stained slices of tissues of Hyalobarrier-treated mice two weeks after induction of peritoneal adhesions. (A) adhesion formed between abdominal wall and cecum. (B) Extensive infiltration of inflammatory cells into mesothelium and smooth muscle of abdominal wall. (C) Adhesion tissue consisting of adipocytes, connective tissue and presence of inflammatory cells. Original magnification of 100x. Arrow indicates inflammatory infiltrate. Ad = adipose tissue, CoT = connective tissue, MI = muscularis, Mu = mucosa, Sm = smooth muscle.

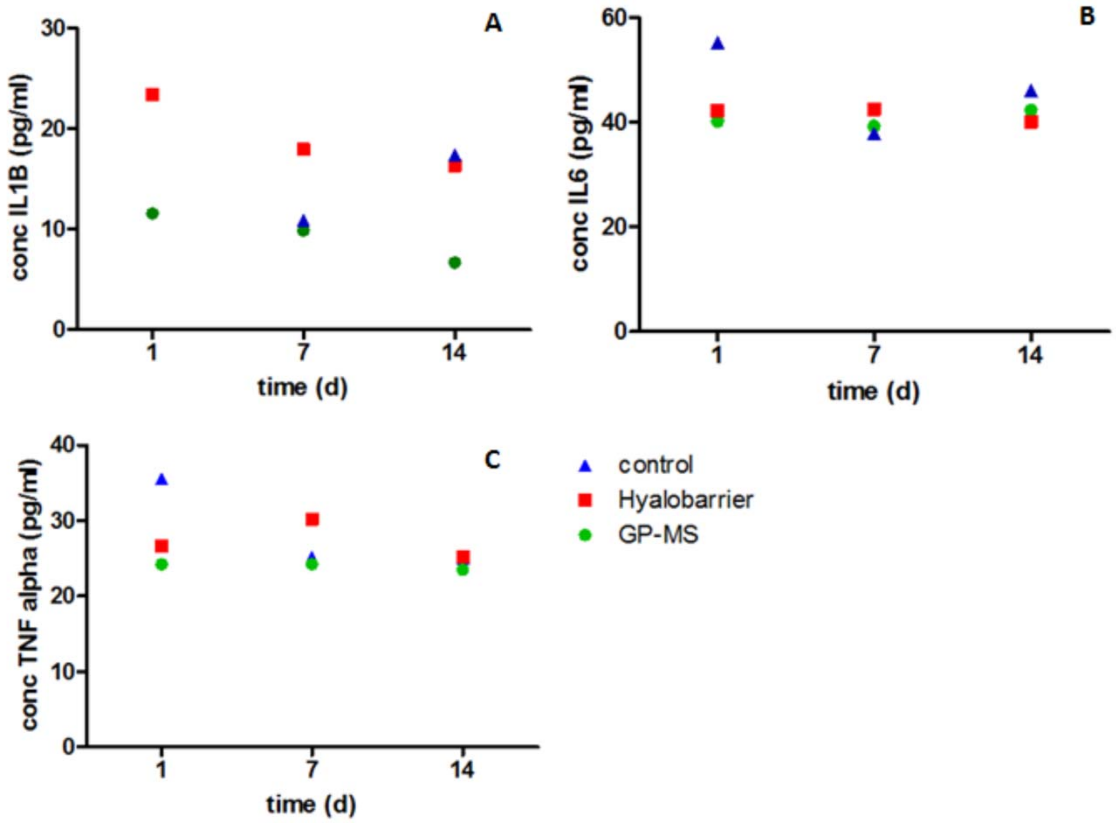

Figure 4: Cytokine evaluation of peritoneal fluid of control, Hyalobarrier and GP-MS-treated mice. Concentration of IL 1B (A), IL 6 (B), TNF alpha (C) in pg/ml are displayed in function of time (day 1, 7 and 14 post-operative).